



**UNIVERSITI PUTRA MALAYSIA**

***DESIGN AND DEVELOPMENT OF ULTRASONIC ACTUATING  
MECHANISM FOR HARVESTING AND PRUNING OPERATIONS IN OIL  
PALM PLANTATION***

**CHIA SIEW LANG**

**Ip  
FK 2020 5**

**DESIGN AND DEVELOPMENT OF ULTRASONIC ACTUATING  
MECHANISM FOR HARVESTING AND PRUNING  
OPERATIONS IN OIL PALM PLANTATION**



**CHIA SIEW LANG**

**189332**

**BACHELOR OF AGRICULTURAL AND BIOSYSTEMS  
ENGINEERING WITH HONOURS**

**FACULTY OF ENGINEERING  
UNIVERSITI PUTRA MALAYSIA**

**2019/2020**

## Approval Sheet

This thesis entitled “**Design and Development of Ultrasonic Actuating Mechanism for Harvesting and Pruning Operations in Oil Palm Plantation**” prepared and submitted by **Chia Siew Lang** as fulfilment of requirements for the degree of Bachelor of Agricultural and Biosystems Engineering with Honours has been examined and is recommended and acceptance.

Approved by:

..... Date: .....

(Dr. Sharence Nai Sowat)  
Project Supervisor

Approved by:

..... Date: .....

(Prof. Madya Dr. Nazmi Bin Nawi)  
Project Examiner

Approved by:

..... Date: .....

(Dr. Anas Bin Mohd Mustafah)  
Project Examiner

## **Acknowledgement**

I would like to take this opportunity to express my appreciation and thanks to individuals and institutions for their continuous support and encouragement to make this project to be completed successfully. A special thanks to Universiti Putra Malaysia and the Department of Biological and Agricultural Engineering for providing this learning opportunity. My sincere thanks to my supervisor, Dr. Sharence Nai Sowat and Coordinator of Final Year Project Dr. Mohd Nazren Bin Radzuan for guiding, supporting and encouraging me in completing this project. I would also like to spend my greatest appreciation and thanks to all my friends who had spent a lot of time together and supporting each other. Lastly, I would like to express my deep gratitude to my parent who had strongly gave support throughout this period. Once again, my heartfelt thanks to everyone.

## Abstract

This project carried out the design and development of ultrasonic actuating mechanism for oil palm trimmer. The focus of this project was selecting the suitable horn design and determining the frequency required for frond trimming. Performance of a horn depends on its physical properties of material and its geometry. Three horns: Stepped horn, Exponential horn, and Catenoidal horn were fabricated for testing. Calculation analysis of the horns was used to determine the performance of each horn. The amplification factor of stepped horn, exponential horn and catenoidal horn was 2, 1.202 and 1.513 respectively. Horn tuning shows that the difference of natural frequency between the horn and transducer was 2.59 (stepped horn), 1.95 (exponential horn) and 1.54 (catenoidal horn). The most suitable horn for amplitude amplification was catenoidal horn due to its combination of good amplifying and stress distribution characteristics. Moreover, horn tuning of catenoidal horn shows that it has nearest resonant frequency to the actuator which indicates that it has the best vibration transmission performance among three horns. The frequency and amplitude of vibration were calculated from the maximum cutting force required for oil palm frond cutting. The result shows that the frequency was inversely proportional to vibration amplitude and the cutting force requirement was inversely proportional to the frequency.

## Abstrak

Projek ini menjalankan reka bentuk dan pembinaan mekanisme penggerak ultrasonik untuk pemotong kelapa sawit. Fokus projek ini adalah untuk memilih reka bentuk horn yang sesuai dan menentukan frekuensi yang diperlukan untuk memotong pelepah kelapa sawit. Prestasi horn bergantung kepada sifat fizikal bahan dan bentuk geometrinya. Tiga horn: horn stepped, horn exponential dan horn catenoidal difabrikasi untuk diuji. Analisis pengiraan digunakan untuk menentukan prestasi setiap horn. Faktor amplification horn stepped, horn exponential and horn catenoidal adalah 2, 1.202 dan 1.513 masing-masing. Penalaan horn menunjukkan perbezaan natural frekuensi antara horn dengan transduser adalah 2.59 (horn stepped), 1.95 (horn exponential) dan 1.54 (horn catenoidal). Horn yang paling sesuai untuk meningkatkan amplitud adalah horn catenoidal kerana gabungan ciri-ciri penguatan amplitud dan taburan tekanan yang baik. Tambahan lagi, penalaan horn catenoidal menunjukkan bahawa ia mempunyai frekuensi resonan terdekat dengan transduser. Ini menunjukkan bahawa ia mempunyai prestasi transmisi getaran terbaik di antara tiga horn. Frekuensi dan amplitud getaran dihitung dari daya pemotongan maksimum yang diperlukan untuk memotong pelepah kelapa sawit. Hasilnya menunjukkan bahawa frekuensi berbanding terbalik dengan amplitud getaran dan keperluan daya pemotongan berbanding terbalik dengan frekuensi.

## Table of Contents

|  |           |
|--|-----------|
| Approval Sheet .....                                   | ii        |
| Acknowledgement .....                                  | iii       |
| Abstract .....   | iv        |
| Abstrak .....  | v         |
| Table of Contents .....                                | vi        |
| List of Tables .....                                   | viii      |
| List of Figures .....                                  | ix        |
| List of Abbreviation .....                             | xi        |
| <b>Chapter 1 Introduction .....</b>                    | <b>1</b>  |
| 1.1 Overview .....                                     | 1         |
| 1.2 Harvesting and Pruning of Oil Palm .....           | 2         |
| 1.3 Mechanization in Oil Palm Harvesting .....         | 3         |
| 1.4 Ultrasonic Cutting .....                           | 4         |
| 1.5 Problem Statement .....                            | 5         |
| 1.6 Objective .....                                    | 6         |
| 1.7 Scope and Limitations .....                        | 7         |
| <b>Chapter 2 Literature Review .....</b>               | <b>9</b>  |
| 2.1 Current Method of Harvesting .....                 | 9         |
| 2.2 Ultrasonic Cutting Device .....                    | 14        |
| 2.3 Ultrasonic Horn .....                              | 18        |
| 2.4 Ultrasonic Transducer .....                        | 21        |
| 2.5 Force Requirement for Oil Palm Frond Cutting ..... | 23        |
| <b>Chapter 3 Methodology .....</b>                     | <b>25</b> |
| 3.1 Design Concept .....                               | 26        |
| 3.2 Ultrasonic Horn Design .....                       | 26        |
| 3.3 Horn Tuning .....                                  | 30        |
| 3.4 Cutting Force Requirement .....                    | 34        |
| <b>Chapter 4 Result and Discussion .....</b>           | <b>40</b> |
| 4.1 Horn Design .....                                  | 40        |
| 4.2 Horn Tuning .....                                  | 48        |
| 4.3 Cutting Force Requirement .....                    | 50        |
| 4.4 Comparison with Current Oil Palm Cutter .....      | 52        |
| <b>Chapter 5 Conclusion and Recommendations .....</b>  | <b>54</b> |

|                                |           |
|--------------------------------|-----------|
| <b>Chapter 6 Summary</b> ..... | <b>55</b> |
| References .....               | xii       |
| Appendices .....               | xv        |



© COPYRIGHT UPM

## List of Tables

|   |       |
|---|-------|
| Table 1: Physical properties of aluminium .....                   | 30    |
| Table 2: Parameters and result of 90o cutting (Jelani, 1998)..... | 39    |
| Table 3: Geometry parameters of horns.....                        | 43    |
| Table 4: Amplification factor.....                                | 45    |
| Table 5: Resonant frequency.....                                  | 48    |
| Table 6: Longitudinal amplitude across stepped horn. ....         | xviii |
| Table 7: Longitudinal amplitude across exponential horn. ....     | xix   |
| Table 8: Longitudinal amplitude across catenoidal horn. ....      | xx    |



## List of Figures

|   |    |
|---|----|
| Figure 1: Cross section of OPF (Bulan et al., 2015).....  | 3  |
| Figure 2: Spring powered sickle cutter (Ahmad & Hitam, 1999).....   | 10 |
| Figure 3: Cantas™ (Jelani et al., 2008).....  | 11 |
| Figure 4: Ckat™.....  | 12 |
| Figure 5: E cutter (Azhar et al., 2012). ....   | 13 |
| Figure 6: Battery-driven cutter (M. R. Ahmad et al., 2020) .....  | 14 |
| Figure 7: Components of ultrasonic cutting system (Sinn et al., 2005).....  | 15 |
| Figure 8: Comparison between the theoretical and experimental friction forces at different cutting speeds (Han, Zhang & Song, 2019) .....                     | 15 |
| Figure 9: Comparison of workpiece surface of (a) conventional cutting and (b) ultrasonic cutting.....   | 16 |
| Figure 10: Chipping during inclined UVC (Jin & Murakawa, 2001).....   | 17 |
| Figure 11: Magnitude of response of ultrasonic transducer (a) without loading (b)with loading (Babitsky et al., 2004) .....                                   | 20 |
| Figure 12: Structure of Langevin Transducer: 1. Matching; 2. Steps of the matching; 3. Double piezoelectric rings; 4. Backing (Karafi & Khorasani, 2019)..... | 21 |
| Figure 13: Relationship between vibration velocity and driving frequency at room temperature(Yamaguchi et al., 2012).....                                     | 22 |
| Figure 14: New terminal mass design of Langevin-type transducer.....  | 23 |
| Figure 15: Project flowchart.....   | 25 |
| Figure 16: Design Concept .....   | 26 |
| Figure 17: Schematic diagram of horn tuning set up. ....  | 31 |
| Figure 18: Horn tuning set up with bare transducer.....   | 32 |
| Figure 19: Stepped horn tuning.....   | 32 |
| Figure 20: Exponential horn tuning. ....  | 33 |
| Figure 21: Catenoidal horn tuning. ....   | 33 |
| Figure 22: Waveform at resonant state. ....   | 34 |
| Figure 23: Force acting on sickle.....  | 35 |
| Figure 24: Force acting on the workpiece.....   | 35 |
| Figure 25: Vibration displacement and velocity of blade edge in feeding direction. ....   | 37 |
| Figure 26: Longitudinal amplitude across stepped horn. ....   | 44 |
| Figure 27: Longitudinal amplitude across exponential horn. ....   | 44 |
| Figure 28: Longitudinal amplitude across catenoidal horn.....   | 45 |
| Figure 29: Amplification factor of horns (1:Stepped horn; 2:Exponential horn; 3:Catenoidal horn).....   | 46 |

Figure 30: Comparison of resonant frequency..... 49  
Figure 31: Stepped horn..... xv  
Figure 32: Exponential horn..... xvi  
Figure 33: Catenoidal horn..... xvii



© COPYRIGHT UPM

## List of Abbreviation

|           |                                     |
|-----------|-------------------------------------|
| $y(x)$    | Longitudinal amplitude              |
| $S(x)$    | Function of cross-sectional area    |
| $w$       | Angular velocity                    |
| $c$       | Longitudinal speed of horn material |
| $f$       | Frequency                           |
| $E$       | Young's Modulus                     |
| $\rho$    | Density                             |
| $s$       | Poisson's ratio                     |
| $\lambda$ | Wavelength                          |
| $L$       | Length                              |
| $M$       | Amplification factor                |
| $A$       | Amplitude                           |
| $s(t)$    | Vibration displacement              |
| $v(t)$    | Vibration velocity                  |
| $t$       | Shear stress                        |
| $z$       | Cutting depth                       |
| $T$       | Period                              |

## Chapter 1 Introduction

### 1.1 Overview

Oil palm is known as one of the major crops in Malaysia. Oil palm as a crop having the highest oil yield among all edible oil crops, its fruits will reach oil content about 40.5% and fibre content about 20% (Macaire et al., 2010) with a considerably high oil to fibre ratio. Palm oil can be consumed as food, commonly more familiar as refined vegetable oil products, as well as biofuel. Over half century, palm oil industry has become a significant contributor to Malaysia's overall economy. According to the Primary Industries Minister Teresa Kok, the total planted area stood at 5.8 million hectares, with more than 19.5 million tonnes of crude palm oil produced in year 2018. The country's total export of palm oil and palm-based products was 25.2 million tonnes, generating export earnings of RM67.5 billion. Meanwhile, the government started the B7 and B10 biodiesel programme which encourage the expansion of oil palm plantation. In-line with the expansion of oil palm plantation, labour requirement of this sector increases as well. Although majority of the labour sources of the oil palm plantation are foreign labour, labour shortage still become a critical issue due to the expenses and the losses caused.

## 1.2 Harvesting and Pruning of Oil Palm

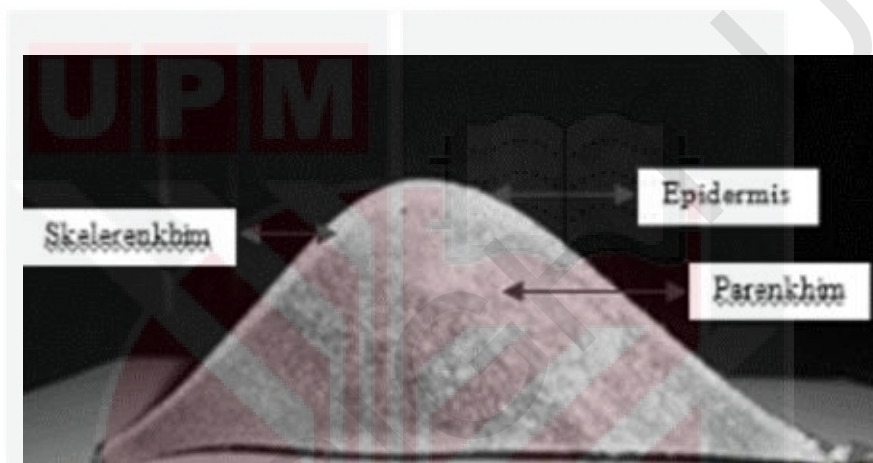
In oil palm plantation, FFB harvesting and collecting activities spend about 30% of the production costs. In order to minimize the expenses, it is crucial for the determination of optimal bunch ripeness for harvesting as well as processing (Rincón et al., 2013). Moreover, palm oil price is dependent on the oil palm FFB quality (Abdullah, Guan, Lim, & Karim, 2004).

The optimum ripeness of FFB able to provide oil extraction rate (OER) higher than 21% and high oil quality which the free fatty acid (FFA) content less than 5% (Abdullah et al., 2004). Ng (1957) mentioned that FFB reaches the maximum FFA level when overripe as such result in poor oil quality. Therefore, it is important that FFB should be harvested at the optimal ripeness in order to achieve maximum OER and ensure high quality oil production.

Besides harvesting, oil palm also requires maintenance from time to time. Pruning of Oil Palm Fronds (OPF) is required to trim the dying leaves and to allow photosynthesis of lower crops. One of the aims of pruning is to improve FFB production. Henson (2002) states that drastic pruning of fronds improves the photosynthesis rate of the remaining fronds on the young palms but only for those with developing bunches. This statement was proved by a statistical result shows that a reduction of fractional interception from 0.91 to 0.22 result of 8 to 40 fronds left in a palm tree after pruning.

As for pruning, determination of OPF mechanical properties aim to develop suitable and effective cutting devices. Hardness of an OPF is determined by the

moisture content in the frond (Bulan, Mandang, & Hermawan, 2015). The study shows that pericarp at an older OPF contains lower moisture than young OPF as a result of the compact fibre structure. This can be explained as the frond grows, more fibrous structures are developed for frond size enlargement thus older fronds tend to be more fibrous (Bulan et al., 2015). Figure 1 shows the cellulose structures of the fronds section.



*Figure 1: Cross section of OPF (Bulan et al., 2015).*

### **1.3 Mechanization in Oil Palm Harvesting**

FFB at optimal ripeness can maximize the oil extraction rate as the bunches having consistent quality and are having maximum oil content at the period (Rincón et al., 2013). The harvesting cycle of oil palm is 15 days, labour shortage during the harvesting and FFB collection process will lead to extension of harvesting period and causes loss of FFB and quality of palm oil.

Besides, manual harvesting using harvesting tools such as chisel and sickle requires workers to be skilful. However, it has become a difficulty for this sector to

get skilled worker especially when the majority of the workers are migrant labour. In order to reduce the labour requirement significantly, the harvesting productivity need a major increase to about 4 tonnes per worker in one day (Jelani et al., 2018). Hence, mechanization in oil palm plantation is necessary to eliminate the use of labour and improve productivity.

Over the years, several mechanized harvesting tools was invented for the harvesting process of oil palm. Malaysia Palm Oil Board (MPOB) has introduced several versions of motorised cutter mainly for harvesting and pruning of palm trees lower than 5m with sickle or chisel cutting head. Motorised cutters are well accepted by the market due to the successful of improving productivity of labour. For taller palm trees, mechanical harvester was introduced to achieve maximum height of 10m. The machine is track-type undercarriage, mounted with cutter and grapple on top of the boom (Shuib, Mohd, Khalid, & Deraman, 2010).

#### **1.4 Ultrasonic Cutting**

Ultrasonic cutting is differed from the conventional cutting in which the cutting edge of the tool is vibrated by ultrasonic wave in the principal or cutting direction which the cutting speed is less than the maximum vibration speed (Jin & Murakawa, 2001). The energy concentration and instantaneous cutting feature of ultrasonic vibration cutting (UVC) enable smaller cutting force and temperature as well as better surface quality by reduces the resistance due to plastic deformation and fracture of material (Han, Zhang, & Song, 2019).

According to several research in UVC technology, the technology was able to improve the cutting experience by reducing friction coefficient, increasing shear angle, working on rigid workpiece, concentrating stress and energy (Han et al., 2019). UVC was proven to be a better cutting mechanism than the conventional ways for a wide range of materials from foods to metals. However, the cutting efficiency of a UVC assembly was dependent on several elements including the blade geometry, the vibration direction relative to the cutting direction, as well as the frequency and amplitude at the cutting edge (Rawson, 1998).

Ultrasonic-assisted cutting has been employed in the wood processing since many years ago. Sinn, Zettl, Mayer, & Stanzl-Tschegg (2005) mentioned that sliding friction forces during cutting was reduced for the ultrasonic-assisted cutting system as the compression forces acted on the workpiece only occur when the cutting edge moving forward to penetrate the workpiece. They also stated that the vibration amplitude must be increased associated with the increasing cutting speed in order to gain an obvious improvement in cutting efficiency.

## **1.5 Problem Statement**

As mentioned above, current harvesting and pruning tool available for short palm trees is motorised cutter. Based on the evaluation of MPOB regarding on the motorised cutter Cantas<sup>TM</sup>, the cutter has low durability on the cutting head, due to frequent breakdown and wearing problems as the result of high speed cutting. Besides, the motorised cutter requires a lot of internal components and mechanisms such as telescopic shaft, bevel gear, and bearings to transmit power from motor to cutting head.

The cutter cannot work even only one of the internal components break down. Thus, the possibility of failure is higher.

Despite its efficiency in cutting FFB and pruning palm tree, however, the high amplitude of vibration has become a weakness that limit the working hour of a worker. As the engine started, high amplitude of vibration was transmitted to the cutting blade along the pole as well as to the operator. According to International Organization of Standardization (ISO5349-1:2001) regarding the measurement and evaluation of human exposure to hand-transmitted vibration, vibration level of  $5\text{m/s}^2$  is a benchmark where the vibration exposures should not exceed the standard. Also, it should not exceed  $2.5\text{m/s}^2$  for daily vibration exposure with maximum 8 hours of exposure duration. High level neurological injuries caused by vibration is incurable due to musculoskeletal damage and muscle fibres deformation, hence lead to pain and different stage of hand disorder (Chowdhry & Sethi, 2017).

Besides, heavy engine which attached at the end of cutter's pole increases the load carried by the operator. For Cantas, the total weight of the cutter is 7.5kg (Jelani et al., 2018) which considerably a heavy load to be portable. Same as the vibration issue, heavy load reduces the labour hour of a worker as it will cause fatigue and pain to the body parts especially arm, shoulder and wrist.

## 1.6 Objective

The main objective of this paper was to design and develop an ultrasonic actuating mechanism for harvesting and pruning operations in oil palm plantation. The

actuating mechanism was designed to reduce the force required for cutting with reduced number of components. Ultrasonic transducer was used to generate resonant frequency vibration to the cutting blade which can provide maximum vibration amplitude and perform improved cutting performance. The mechanism was expected to provide effective cutting with low force requirement and low possibility of failure of the cutting unit.

The more specific objectives would include:

- To analyse and identify the suitable ultrasonic frequency for OPF cutting.
- To analyse and identify the suitable horn design as amplifier for OPF cutter.
- To design and develop an ultrasonic actuating mechanism for oil palm cutter.

High labour requirement and high productivity cost have been the main concerns of the mechanization of oil palm harvesting. Many researches have been done in order to overcome these concerns. Although some mechanized cutters have been developed and are being used currently, but the achievements still cannot fulfil the requirements in all aspects. Ultrasonic cutting which currently widely used in wood processing can be seen as another possibility for the researchers to invent a new version of oil palm cutter.

## **1.7 Scope and Limitations**

In this project, we will focus on the analysis, design and development of ultrasonic actuating mechanism. Various design of ultrasonic horns will be provided

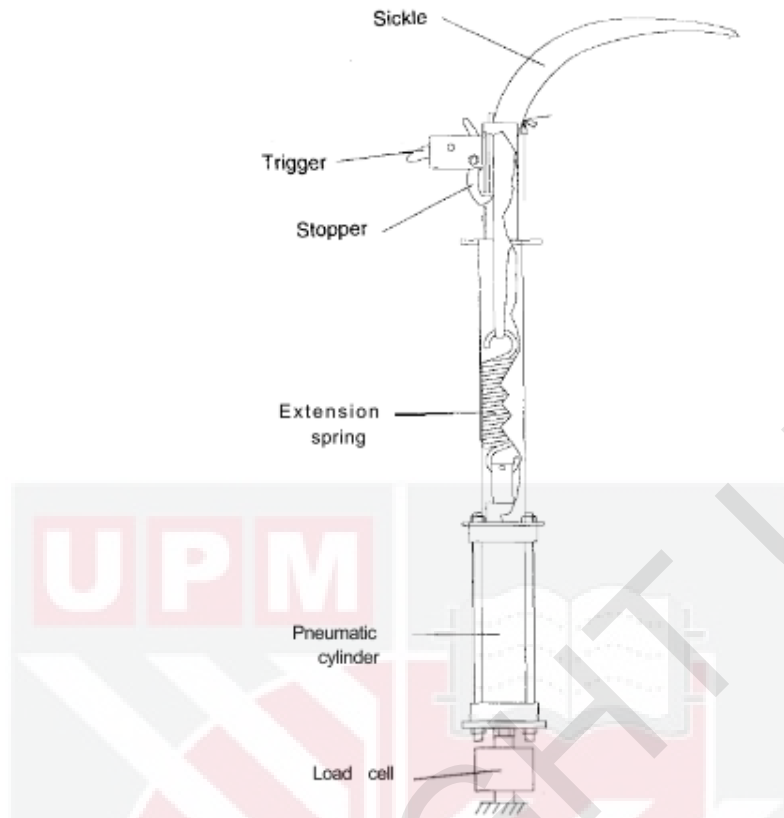
for calculation analysis. The horns will be fabricated for experimental test in lab. Existing ultrasonic transducer available in the market will be used for the testing unit. The performance of each horn design will be compared analytically and experimentally. The most suitable design will be selected for the actuating mechanism. Calculation analysis will be carried out to determine the minimum frequency of the ultrasonic transducer required to generate sufficient cutting force for the actuating mechanism.

One of the limitations of this actuating mechanism is the power supply available by the portable power source such as battery may insufficient to generate power for the transducer. Also, the size and specifications of the piezoelectric transducer decides the power and cutting force developed at the cutting edge. Larger transducer will be needed if the cutting force required to cut OPF is greater, which means that the load being carried by the user will increase as well. Besides, the fabrication of the ultrasonic horn requires longer time and expenses. Limitation of budget and time may limit the development of this actuating mechanism.

## Chapter 2 Literature Review

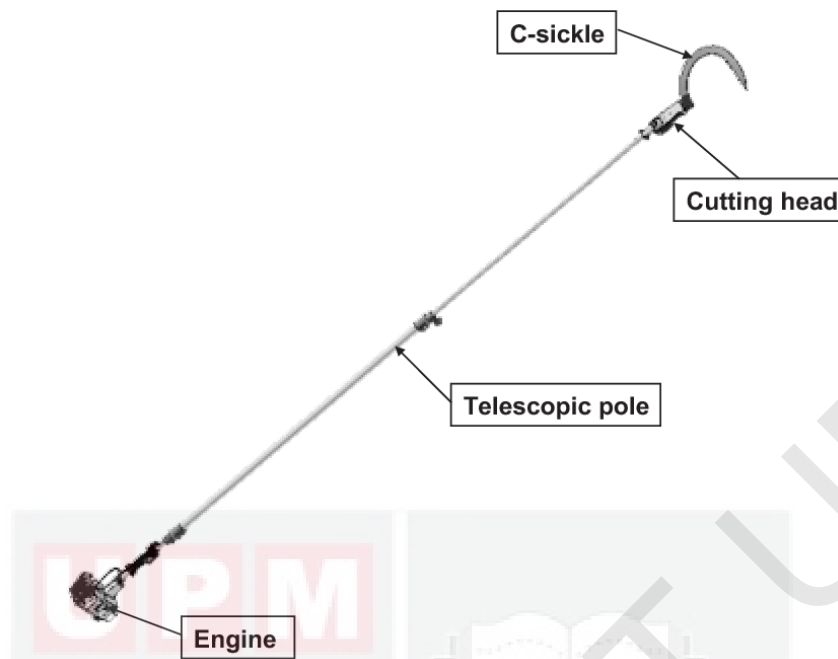
### 2.1 Current Method of Harvesting

The most popular cutting tools for oil palm are sickle and chisel. (D. Ahmad & Hitam, 1999) had designed and developed a spring powered sickle cutter by employing the theory of free cutting where the cutting reaction leads by inertia of static object during high cutting speed. The design of the cutter was a sickle attached to a pole with an extension spring which can provide high cutting speed to overcome resistant of fibre. Moreover, the single direction cutting force eliminates vibration of the tool. However, as stated in the paper, the specific reaction force and energy during cutting are highly depending on the cutting angle by using poled sickle, hence require harvester to be skilful.



*Figure 2: Spring powered sickle cutter (Ahmad & Hitam, 1999)*

C-shaped sickle is the most effective design for cutting and has been widely used in oil palm plantation for harvesting and pruning due to its effectiveness in minimising vibration during cutting (Abdul Razak et al., 2003). Malaysia Palm Oil Board (MPOB) had developed an oil palm cutter for palm trees lower than 4.5m namely Cantas™ with a C-shaped sickle attached to a pole powered by a 1.3hp two-stroke petrol engine. Rotational motion generated by the engine is transmitted via mechanical shaft inside the pole to the gear box. The rotational motion is converted into linear motion at the gear box for linear cutting action.



*Figure 3: Cantas™ (Jelani et al., 2008).*

A study shows that this cutter is effective in cutting and lengthen labour working hours thus improving the FFB harvesting productivity (Jelani et al., 2008). As an additional, perfect skill in handling the cutter can maximize the productivity of the cutter as well (Jelani et al., 2008). This cutter was proven reduce the labour requirement by 50% and improve the FFB harvesting productivity by 176%. Although Cantas™ was well accepted by the market and has been widely used in oil palm plantation, however the sales of the cutter were declining since 2012 due to its less favourable reasons (Jelani et al., 2018). They mentioned the problems found in Cantas™ including short lasting of cutting head due to wear and tear caused by high speed movement, heavy weight, and also high vibration induced to user.

Cantas Evo was modified by adding double bearing system, reducing stroke distance, adding shaft guider and improving strength on connecting rod in order to

improve stability and reduce vibration. Lighter pole material: carbon fibre and lighter motor were used to reduce total weight of the cutter. The cutter was reported reduce the maintenance cost significantly by almost 90% as compared to the previous version (Jelani et al, 2018).

Another motorised cutter was developed by MPOB in 2008 using the same engine and operating design, but replaces the cutting head with a chisel. This motorised cutter named Ckat<sup>TM</sup> was designed mainly for harvesting short palm trees lower than 8m. The average harvesting productivity of FFB using Ckat<sup>TM</sup> has an obvious improvement of 45% higher than that of manual harvesting (Jelani et al, 2008). Since Ckat<sup>TM</sup> employed the same design as Cantas<sup>TM</sup>, it may face the same problems that occurred to the first generation of Cantas<sup>TM</sup> as well.



*Figure 4: Ckat<sup>TM</sup>*

Azhar et al. (2012) had designed a new version of cutter so called E cutter which employed an electrical generator to the original Cantas<sup>TM</sup> design. For E cutter,

a mobile electrical generator was attached on the engine for conversion of energy from mechanical to electrical and a linear actuator was used to provide linear vibration which is relatively less rubbing impact on the cutting blade. Copper wire was used for energy transmission instead of shaft thus enable the tool to operate even when the pole bends due to gravity. However, the linear actuator selected for the design has heavy weight and will cause fatigue if carried for long time.

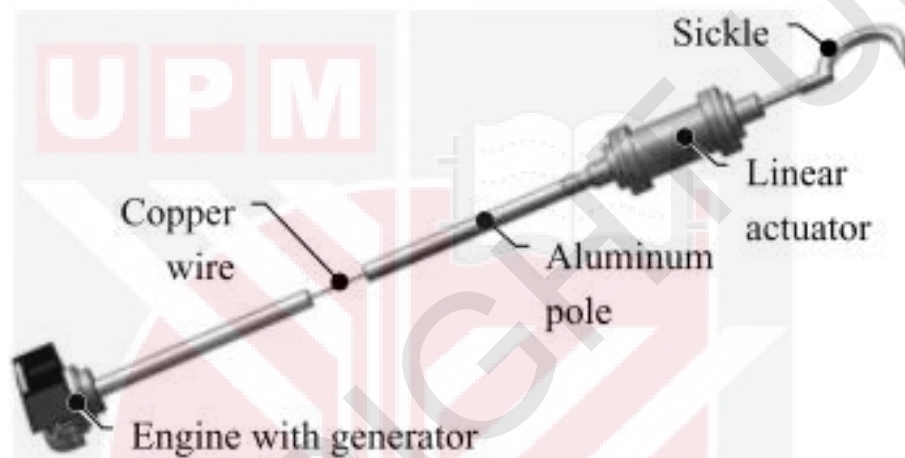


Figure 5: E cutter (Azhar et al., 2012).

A battery powered oil palm cutter namely Cantas Elektro was developed by MPOB/UKM in 2020. The cutting head consists of a sickle and a gearbox. The sickle was driven by an electric motor with the specification of 9700 RPM and a 18V lithium-ion (direct current) battery was used to activate the whole machine system. The cutting head movement depended on the motor electric where the power from electric was transferred by aluminium shaft along inside the pole. The rapid cutting motion of the sickle is in the range of 5000 to 6000 RPM (M. R. Ahmad et al., 2020).



*Figure 6: Battery-driven cutter (M. R. Ahmad et al., 2020)*

## **2.2 Ultrasonic Cutting Device**

Ultrasonic vibration has been employed in industrial machining due to its effectiveness of work as compared to the conventional machining. As for cutting, the basic components made up an ultrasonic cutting system are ultrasonic transducer, ultrasonic horn and blade. Piezoelectric elements in ultrasonic transducer elongate and contract, causing the longitudinal vibration of the tool as shown in figure 7. At resonance, maximum amplitude of vibration can be reached with minimum power input (Sinn et al., 2005).

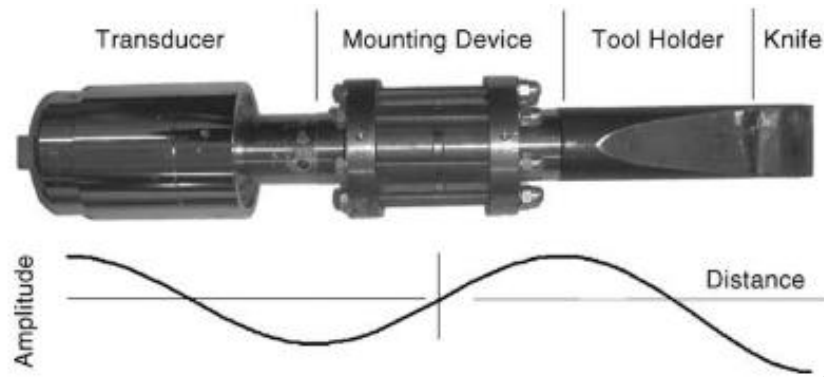


Figure 7: Components of ultrasonic cutting system (Sinn et al., 2005)

Reduction of cutting force is one of the main concerns for a cutting process. Ultrasonic vibration cutting (UVC) reduces cutting force by separation and pulse cutting thus minimising friction between cutting edge and workpiece (Mitrofanov, Babitsky& Silberschmidt, 2003). Durability of UVC cutting head can be lengthen at least five times longer than the conventional cutting tools by restraining the wear and tear effect on the tool (Cheng et al., 2007). Figure 8 shows the increasing friction force due to increasing cutting speed. Thus, wearing of cutting edge will be more severe for high speed cutting tools.

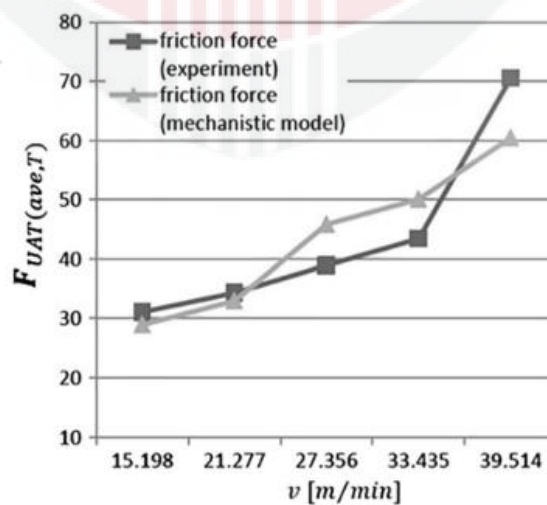
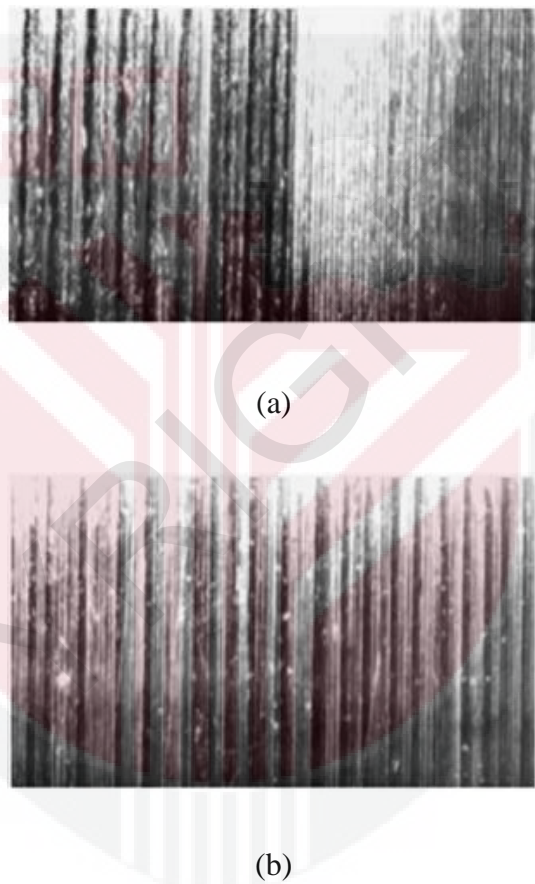


Figure 8: Comparison between the theoretical and experimental friction forces at different cutting speeds (Han, Zhang& Song, 2019)

Yang & Lu (2007) states that high amplitude of cutting tool in UVC enable low net displacement and dimension error on workpiece. This means that UVC able to provide better surface quality. Figure 9 shows the comparison of workpiece surface of conventional cutting and ultrasonic cutting. Cutting surface of ultrasonic cutting system is obviously smoother and more even than the conventional cutting system.



*Figure 9: Comparison of workpiece surface of (a) conventional cutting and (b) ultrasonic cutting.*

Chipping is another consideration for cutting process. Chipping occurs mainly due to friction between cutting edge and the workpiece surface causes cutting force acting in reverse of the feeding direction subsequently and tensile strength acting around cutting edge. A study by Jin & Murakawa (2001) stated that during orthogonal

cutting, inclined vibrating direction from the principal cutting direction of a  $45^\circ$  reducing the contact area between the sides of cutting head and workpiece as such reduce chipping of workpiece.

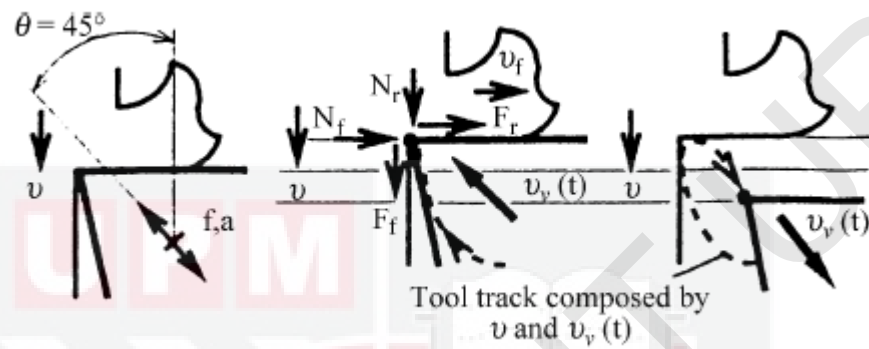


Figure 10: Chipping during inclined UVC (Jin & Murakawa, 2001)

On the other hand, Schneider, Zahn, & Rohm (2008) proposed that as the cutting depth increases, maximum vibration speed increases consequently decreasing the cutting force, but the power output of sonotrode for each unit of contact area between the cutting sides and the workpiece declined as the cutting depth increases. They also mentioned that vibration power required for cutting is highly dependent on the material of workpiece, as for porous materials, lower cutting forces are required for workpiece separation thus lower power required. By relating this point of view to the OPF properties, fronds with lower fibre compact bundle appears to be more porous and hence require smaller cutting force.

A study on the ultrasonic food cutting shows that the maximum cutting force increased significantly as the cutting speed increases without considering the

ultrasonic vibration magnitude (Zahn, Schneider, & Rohm, 2006). In addition, cutting work shows a significant decrement when the maximum vibration speed increased (Zahn et al., 2006). Hence, cutting force of an ultrasonic cutting tool is highly dependent on the cutting speed as well as maximum vibration speed of the ultrasonic support.

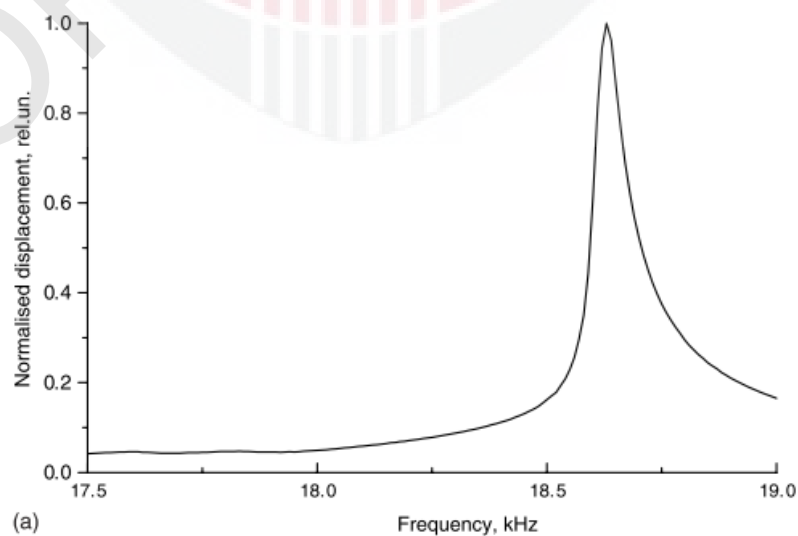
### **2.3 Ultrasonic Horn**

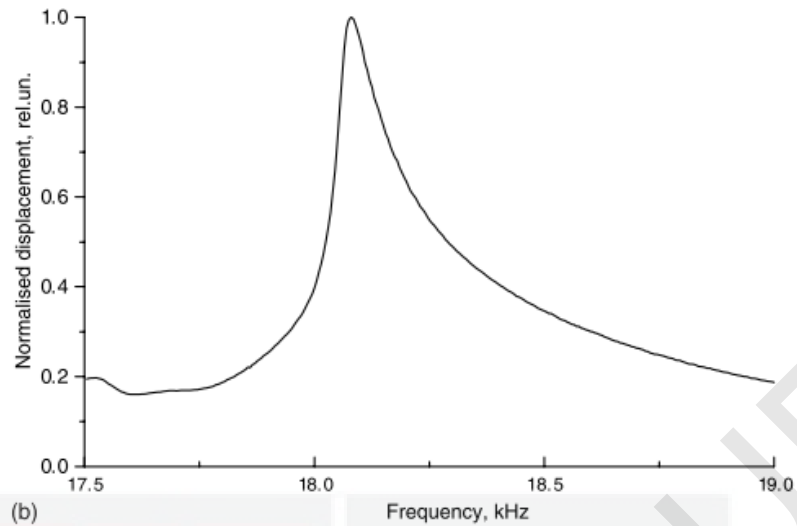
Ultrasonic horn is one of the components of ultrasonic machining assembly as transmission element whether to transmit vibration from transducer to working tool or direct to working material. When the cutting system is operating under load, the amplitude of vibration will drop due to energy loss during interaction of cutting edge and workpiece (Schneider et al., 2008). In this case, a horn plays an important role in amplifying the vibration amplitude.

Ultrasonic cutting requires high amplitude vibration to perform sufficient cutting force. However, high amplitude vibration transmitted to cutting blades generates high stress level on the blade thus leads to frequent breakdown of cutting head. Short blades are therefore more recommended for ultrasonic cutter assembly as the vibration performance in short blades is relatively more controllable than the long blades and is more uniform in vibration transmission (Lucas, Petzing, Cardoni, & Smith, 2001). Suitable horn geometry can ensure good distribution of stress as such reduce the risk of breakdown of cutting tip.

An ultrasonic horn design should concern about the isolation of vibration frequency, the uniformity of amplitude transmission and the magnitude of amplitude during operation. For ultrasonic cutter, horn design is especially important to ensure longitudinal vibrating direction of the cutting head and sufficient vibration transmitted for efficient cutting (Cardoni & Lucas, 2002).

Transmission efficiency of an oscillating system is especially sensitive to loading, for instance, detachable horn or cutting heads which cause losses in energy during transmission (Babitsky, Kalashnikov, & Molodtsov, 2004). For this reason, the peak performance of an ultrasonic machining system could never be reached, however, the actual steady state of the system can be investigated through frequency tuning (Babitsky et al., 2004). The resonant frequency of the tuned horn can be used as a parameter for the selection of horn. Ideal horn should have small difference of resonant frequency as possible to reduce the effect of loading to the energy transmission from the transducer to cutting tip. As shown in figure 11, the magnitude of response of ultrasonic transducer with loading is significantly lower than the unloaded transducer.





*Figure 11: Magnitude of response of ultrasonic transducer (a) without loading (b) with loading (Babitsky et al., 2004)*

Resonant frequency of a horn is affected by the horn material and the geometry of the horn. Mechanical properties of the horn material such as elasticity and density affect the transmission speed of acoustic vibration across the horn. Ideal length of an acoustic horn to perform good amplification should be equal to half of the wavelength of the horn material (Nad, 2010). The factor amplification of mechanical strain is the ratios of input and output diameters (Pérez-Sánchez, Segura, Rubio-Gonzalez, Baldenegro-Pérez, & Soto-Cajiga, 2020). Hence, the strain performance of the horn can be increased by varying the diameter of output end, where the cutting tool was connected to. There are also some cases where the horn and cutting edge are fabricated in one piece. In this case, the dimension of the cutting edge will affect the strain performance of the horn.

Common designs of acoustic horns are stepped horn, exponential horn, taper horn etc. The shape and geometry of the horn determine its amplifying performance and stress distribution. The performance of stepped horn depends on the location of

step, where the diameter change, whereas, horns with taper or concave design depend on the inclined angle and the curvature (Nad, 2010).

## 2.4 Ultrasonic Transducer

Ultrasonic transducer act as an actuator in generating ultrasonic vibration for all ultrasonic machining. Langevin transducers are often used in high power application. A basic structure of ultrasonic transducer would include a backing metal, double piezoelectric rings, and a matching (figure 12). For applications that having small mechanical load yet working in large vibration amplitude such as cleaning, the transducer tends to overheat due to power losses, result in poor resonance performance and low durability in piezoelectric rings (Karafi & Khorasani, 2019). However, for ultrasonic cutting, the mechanical load faced by the transducer is much greater than ultrasonic cleaning. Therefore, it is expected to have lower chances of overheat of transducer in ultrasonic cutting.

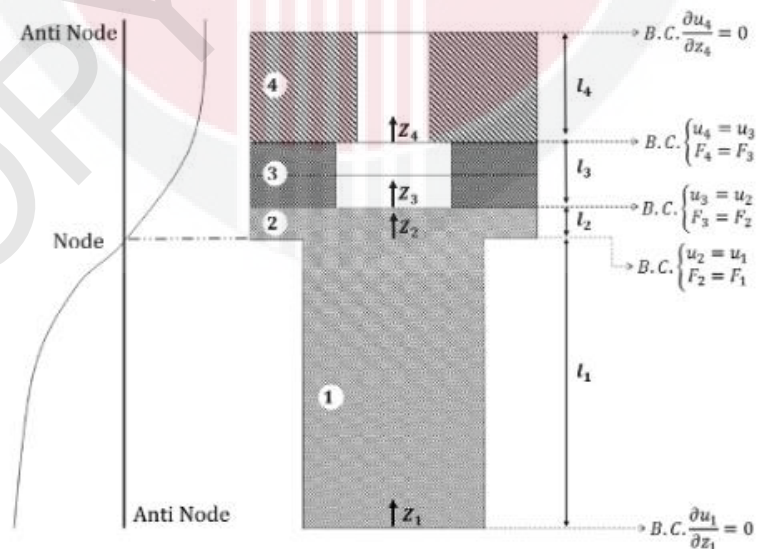


Figure 12: Structure of Langevin Transducer: 1. Matching; 2. Steps of the matching; 3. Double piezoelectric rings; 4. Backing (Karafi & Khorasani, 2019)

Langevin type transducers are often used in ultrasonic cutting as they can produce great force and low heat production. A study on fabrication of ultrasonic transducer for cryogenic temperature shows that bolt-clamped Langevin transducer can overcome temperature stress and able to perform high level of vibration. In the study, a sinusoidal voltage of  $90^\circ$  phase difference was applied to each quartered electrode in order to create two bending vibration modes perpendicularly. The evaluation of the transducer shows that when a  $50V_{p-p}$  voltage was applied, the driving frequency was  $76.10\text{kHz}$  and the maximum vibration velocity was  $236\text{mm/s}$  as shown in figure 13 (Yamaguchi, Kanda, & Suzumori, 2012). The vibration frequency can be varied by varying the voltage supply. Lower voltage applied at similar driving frequency results in lower vibration frequency.

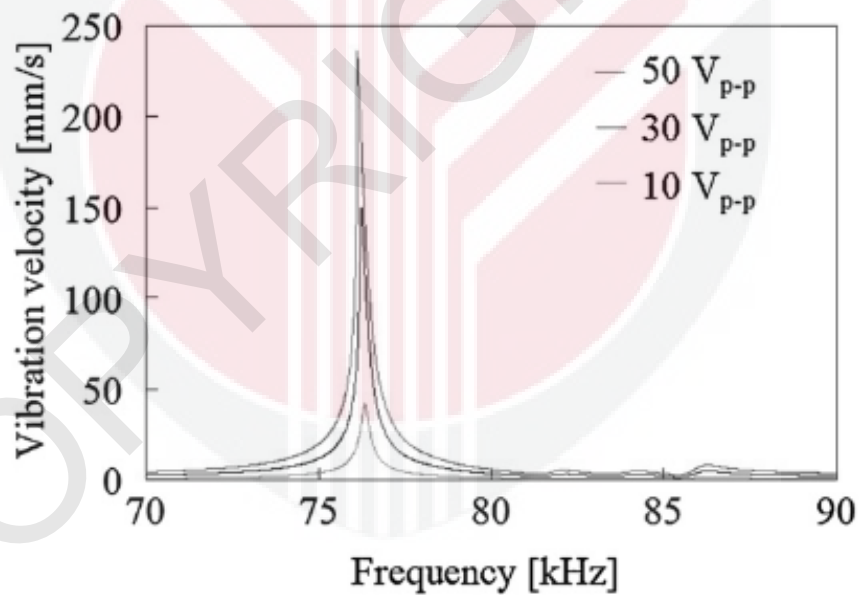
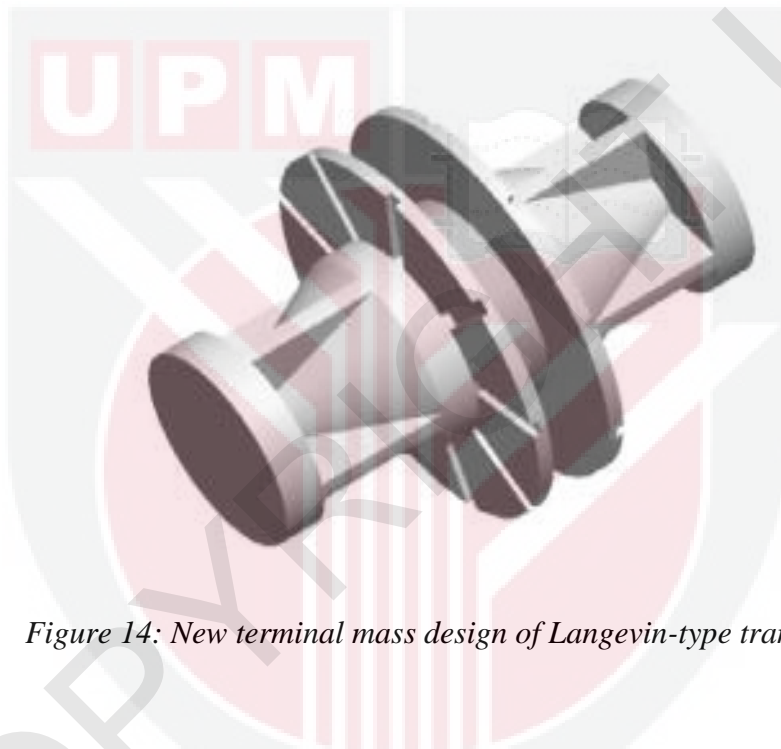


Figure 13: Relationship between vibration velocity and driving frequency at room temperature (Yamaguchi et al., 2012)

The characteristics of terminal mass attached to the piezoceramic disc affects vibration performance of an ultrasonic transducer. Lu, Hu, Peng, & Wang (2017)

proposed a new topological design of Langevin-type transducer. The new Langevin transducer (MOLT) differ from the conventional Langevin transducer (TLT) in terms of the terminal mass block design. The comparison of finite analysis of both Langevin transducer shows that MOLT has generates higher amplitude than TLT. This is due to the lighter mass of MOLT generates greater energy than TLT for the same voltage input as energy losses during the vibration transmission is reduced according to the reduced mass structure.



*Figure 14: New terminal mass design of Langevin-type transducer.*

## **2.5 Force Requirement for Oil Palm Frond Cutting**

As described in (Jelani et al., 2008), fibre and cellulose structure of OPF and FFB stalk are important considerations to design an effective oil palm cutter. Hardness of OPF varies from inside to outer surface of fronds. Darwis, Massijaya, Nugroho, Alamsyah, & Nurrochmat (2014) mentioned that the bottom part of oil palm fronds shows the strongest mechanical properties as compared to the upper part of trunk. Hence, cutting tools often fails at the bottom part of the fronds.

The factors affecting the mechanical strength of OPF are frond maturity, moisture content, and the section of cutting. Mature fronds tend to have higher mechanical strength due to the fibrous structure. High moisture content of fronds causes the firmness of the fibrous material (Mandang, Sinambela, & Pandianuraga, 2018). The frond section nearest to the trunk requires the highest cutting force due to the high moisture content and high fibrous structure. Both maturity and moisture content of OPF having effect on the cutting force. However, moisture content shows more significant effect on the cutting force in shear test. The maximum shear load for section nearest to trunk with high level of moisture and maturity is 2900N (Alnuami, Janius, & Ahmad, 2015).

Sickle cutter is the most suitable cutting tool for OPF trimming as it performs slicing cut. Same with normal cutting, cutting angle plays an important role in reducing force requirement during OPF cutting. The greater the inclined angle, the smaller the force required for cutting. Hence, actual cutting of OPF requires the operator to bring the cutter near to the palm's trunk. Cutting force required to cut high maturity OPF is maximum at 90°, which is normal to the cutting plane of the frond (Jelani et.al, 1998).

### Chapter 3 Methodology

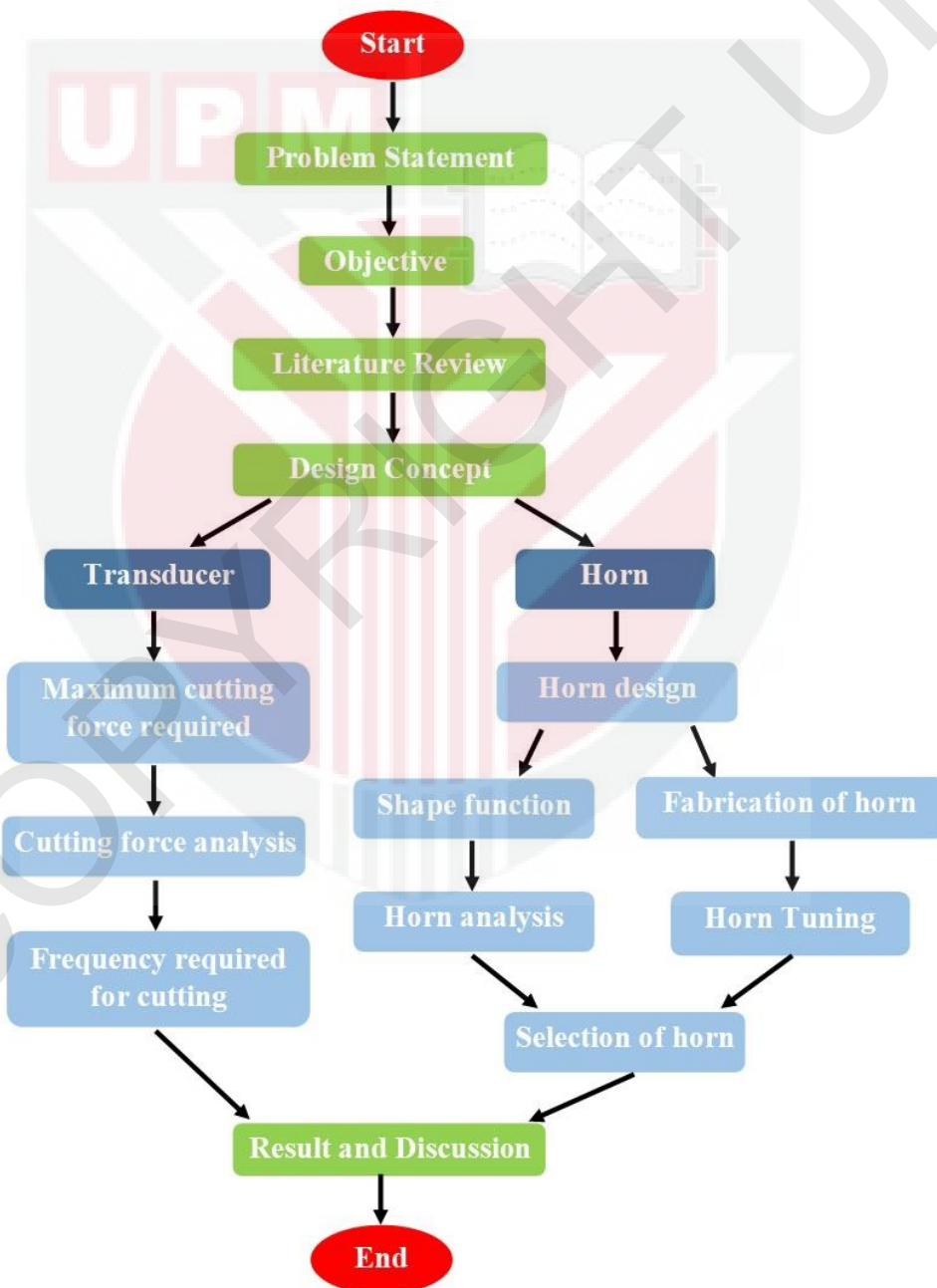


Figure 15: Project flowchart

### 3.1 Design Concept

A few mechanised cutters were developed for harvesting and pruning in oil palm plantation. Most of the cutters are developed with a cutting head (chisel or sickle) attached to a pole and cutting through vibration on the cutting head which powered by engine or electrical generator. In this design, the cutting head will be attached to a pole similar to other cutters, however the vibration and power supply will be replaced with an ultrasonic transducer powered by AC power supply. The design concept was shown in figure 16.

When the piezoelectric element in the transducer is applied with AC voltage aligned with its frequency, resonance occur. Resonance phenomenon allow small force to achieve large oscillation. The vibration generated by the ultrasonic transducer is transmitted to cutting head through an ultrasonic horn causing the cutting head to perform oscillation at maximum amplitude.

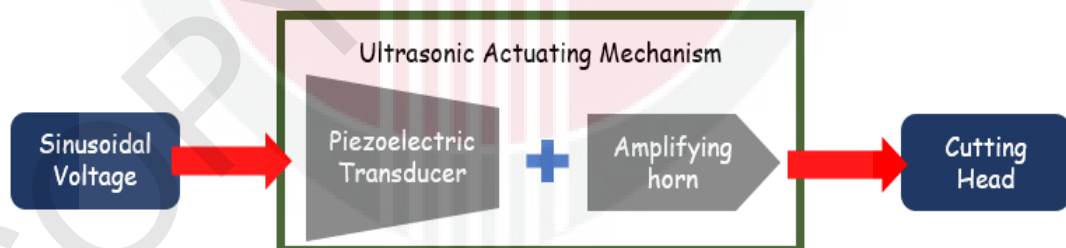


Figure 16: Design Concept

### 3.2 Ultrasonic Horn Design

An ultrasonic horn will be connected to an ultrasonic transducer with a connecting bolt. Shorter horn design is more favourable to reduce energy loss during vibration transmission (Lucas et al., 2001). However, horn length is not the only

consideration of its efficiency in transmitting vibration. Geometries and the natural frequencies of the horns also affect the loading effect. Hence, in order to determine the most suitable horn design for the ultrasonic transducer, experiment will be done on several horn design by testing the frequency required to achieve resonance when loading is added to the transducer.

The transducer is connected to a signal generator and an oscilloscope for horn tuning. The signal generator generates repetitive sinusoidal waveform to the ultrasonic transducer while the oscilloscope analyses and display the waveform of the transducer. The resonant frequency of the transducer itself as well as when loading added are determined by tuning the signal generator. During resonance, the resonant frequencies should be approximately equal to the natural frequency of the transducer whether loaded or unloaded. The horn design which require smallest power and resonant frequency will be selected.

Ultrasonic horn act as an amplifier to amplify the amplitude of vibration from the transducer. The performance of a horn depends on its dimensions, geometry and what material it is made from. According to an acoustic horn analysis done by Amin, Ahmed, & Youssef (1995), the design of ultrasonic horn is based on the equilibrium of an infinitesimal element under elastic action, inertia forces, and integration over the horn length to attain resonance. The equilibrium function can be expressed as the equation below:

$$\frac{d^2y}{dx^2} + \frac{d \ln S(x)}{dx} \frac{dy}{dx} + \frac{\omega^2}{c^2} y = 0 \quad (1)$$

where  $y$  is the amplitude of longitudinal vibration,  $S(x)$  is the function of cross-sectional area along the length of the horn,  $x$ ,  $\omega$  is the angular velocity, and  $c$  is the longitudinal speed of the horn material.

The angular velocity is the rate of change of waveform phase in the oscillation.

It can be obtained from the equation:

$$\omega = 2\pi f \quad (2)$$

where  $f$  is the resonant frequency.

The longitudinal sound velocity of the horn material can be expressed as:

$$c = \sqrt{\frac{E}{\rho}} \quad (3)$$

where  $E$  is the Young's Modulus of elasticity and  $\rho$  is the density of the horn material (Amin et al., 1995).

However, the equation described above does not take the elastic properties of the horn material into account (Pérez-Sánchez et al., 2020). This may causes the value obtained differ from the actual value. By taking the elastic properties into account, the longitudinal sound velocity of the horn can be expressed in the following equation:

$$c = \sqrt{\frac{E}{\rho} \frac{1 - \sigma}{(1 + \sigma)(1 - 2\sigma)}} \quad (4)$$

where  $E$  is Young's Modulus of elasticity,  $\rho$  is the density of the horn material, and  $\sigma$  is the Poisson's ratio.

The length of the ultrasonic amplifier should be half of its wavelength (Vivekananda, Arka, & Sahoo, 2014):

$$L = \frac{\lambda}{2} \quad (5)$$

According to basic principal of wave, the relationship of the wave velocity, frequency and wavelength can be described as  $c = fl$ , where  $c$  is the longitudinal sound velocity,  $f$  is the resonant frequency, and  $l$  is the wavelength of oscillation. Hence, the length of the horn can also be expressed as:

$$L = \frac{c}{2f} \quad (6)$$

The performance of the ultrasonic horn can be evaluated in terms of amplification factor, which shows the amplification of mechanical strain according to the ratio of the amplitude of both ends of the horn (Nad, 2010):

$$M = \left| \frac{A_{out}}{A_{in}} \right| \quad (7)$$

where  $A_{in}$  and  $A_{out}$  are amplitudes of the input and output ends of the horn.

In a nutshell, the resonant frequency of the horn depends on its dimension, geometry, and physical properties of material (Pérez-Sánchez et al., 2020). The dimension and geometry affect the amplifying properties and the stress distribution of

the horn whereas the physical properties of the material such as density affects the vibration transmission across the horn.

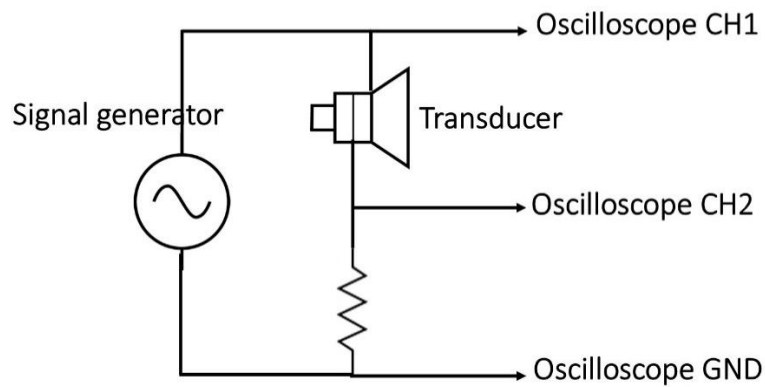
For testing purpose, three ultrasonic horns of different design were fabricated. Material used to fabricate the horns was aluminium. The physical properties of aluminium are:

| <b>Young's Modulus, <math>E</math><br/>(GPa)</b> | <b>Density, <math>\rho</math> (kg/m<sup>3</sup>)</b> | <b>Poisson's Ratio, <math>\nu</math></b> |
|--|--|--|
| 69   | 2700   | 0.334                                    |

*Table 1: Physical properties of aluminium*

### **3.3 Horn Tuning**

The horns tuning experiments were carried out in order to determine the resonant frequency of each horn design. The performances of the horns were observed to determine the most suitable horn design for amplifying the ultrasonic transducer vibration. A 60W 28kHz Langevin type ultrasonic transducer was purchased for testing. Each horn was connected to the Langevin transducer using a couple stud. The assembly was connected to an oscilloscope and a frequency generator. The connection of the circuit was shown in figure 17 and the experiment set up was shown in figure 18-21.



*Figure 17: Schematic diagram of horn tuning set up.*

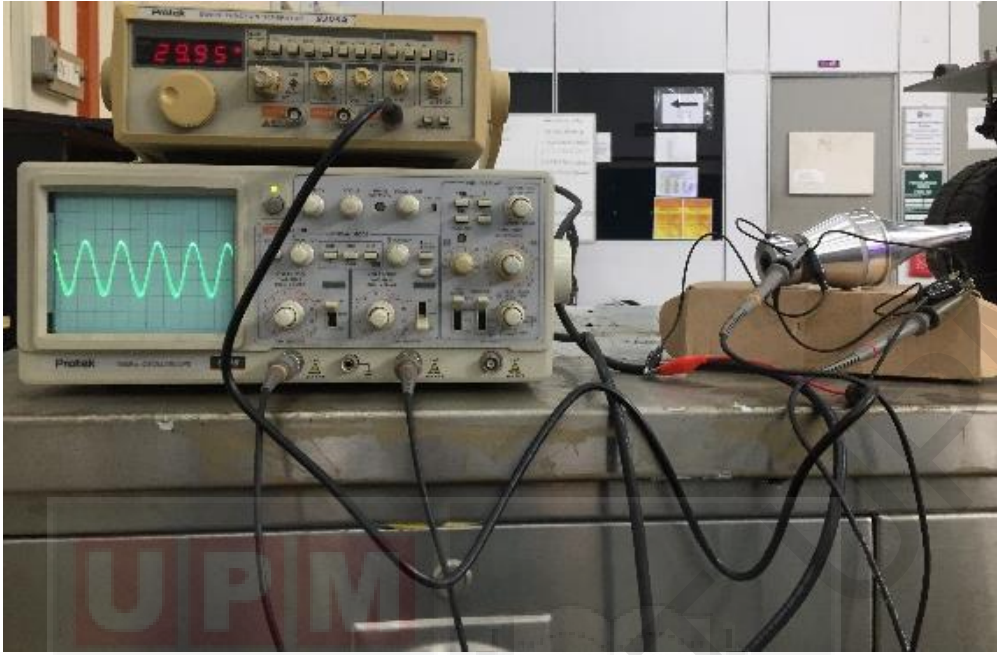
Protek 9205A Sweep Function Generator and Protek 6510 100MHz Oscilloscope were used to tune the horns. The experiment was started with the bare transducer. This is to determine the natural frequency of the ultrasonic transducer without load. The frequency generator was adjusted while observing the waveform shown in oscilloscope display. The setting was tuned until the resonant state. Figure 22 shows the wave pattern during resonant state. The frequency generated by the generator at this moment was the resonant frequency, which provide maximum amplitude of vibration. The experiment was then continued by connecting each horn to the Langevin transducer. The resonant frequency of each horn was observed and recorded.



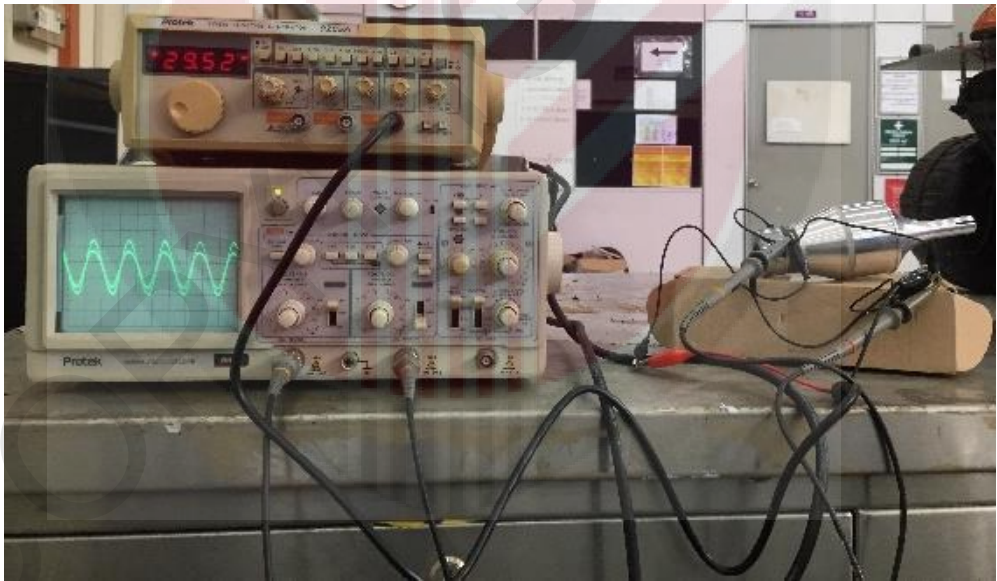
Figure 18: Horn tuning set up with bare transducer



Figure 19: Stepped horn tuning.



*Figure 20: Exponential horn tuning.*



*Figure 21: Catenoidal horn tuning.*

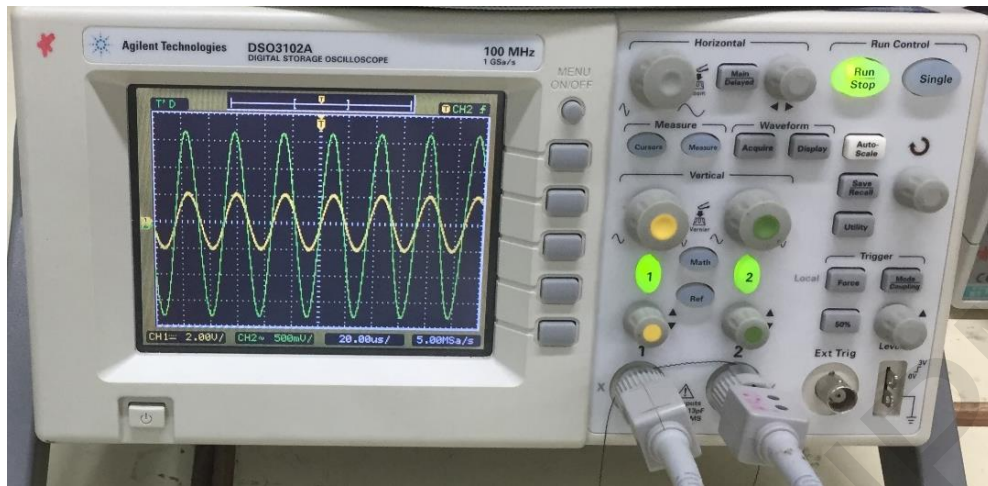


Figure 22: Waveform at resonant state.

### 3.4 Cutting Force Requirement

The force acting on the sickle during cutting process was illustrated in figure 23 which shows that the direction of cutting force is parallel to the direction of cutting motion. The force acting on the workpiece was illustrated in figure 24, where x-axis is the direction parallel to the cutting surface and y-axis is the direction normal to the cutting surface.

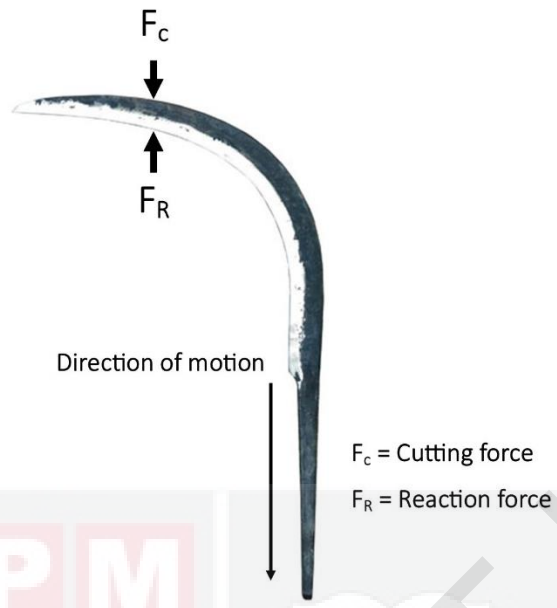


Figure 23: Force acting on sickle.

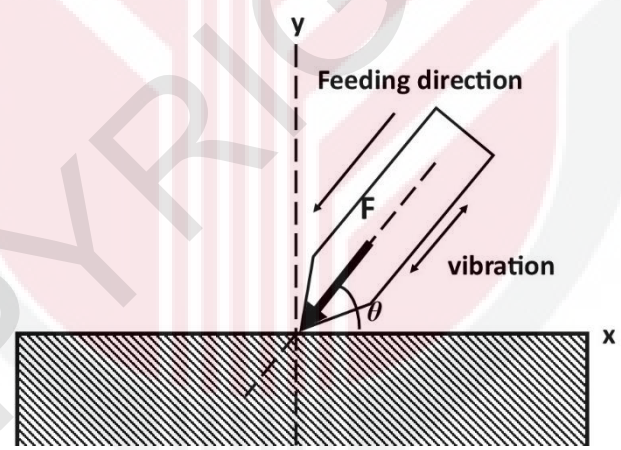


Figure 24: Force acting on the workpiece.

When ultrasonic vibration is induced from the transducer to the blade, the blade will vibrate at a frequency and an amplitude corresponding to the transducer performance. The vibration of the blade edge can be illustrated in sinusoidal waveform as shown in figure 25. Since the direction of vibration is parallel to the feeding direction, there will be no effect of inclined angle to the blade displacement. The total

displacement of the blade is the sum of the displacement due to ultrasonic vibration and the feeding motion. Hence, the displacement and velocity of the blade edge in the feeding direction can be expressed as (Dong, Anish, & V, 2020):

$$s(t) = A \cos 2\pi ft + vt \quad (8)$$

$$v(t) = -2\pi fA \sin 2\pi ft + v \quad (9)$$

where  $x$  and  $y$  are direction parallel and normal to the cutting plane respectively.  $v$  refers to the cutting speed of cutter in the feeding direction, and  $\theta$  refers to the angle between the cutting plane and the blade axis.

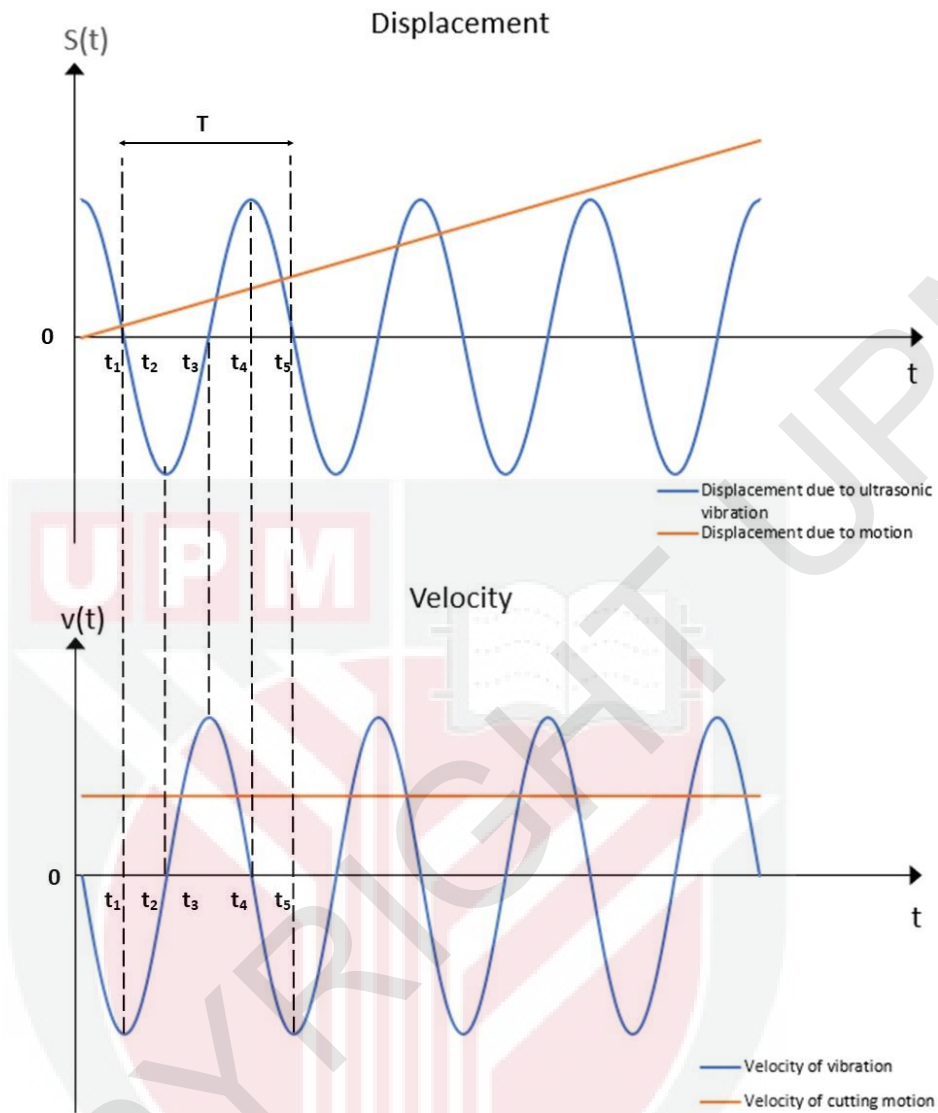


Figure 25: Vibration displacement and velocity of blade edge in feeding direction.

According to Hu, Yu, Li, & Chen (2017), cutting force can be defined as the penetration force required by the cutting edges to overcome the damage resistance of the workpieces and provide separation as required. Different from conventional cutting, cutting force during ultrasonic assisted cutting is no longer a constant value. The ultrasonic transducer induces vibration at certain amplitude and frequency, causes the tool edges to be in contact with and separate from the workpiece alternatively for the whole cutting process.

As illustrated in figure 25, the blade is moving downward from  $t_0$  to  $t_2$  and moving upward from  $t_2$  to  $t_4$ . The blade edge penetrates into the workpiece in between  $t_1$  to  $t_3$  and separated from the workpiece in between  $t_3$  to  $t_5$ . Corresponding to the displacement, the vibration velocity of blade edge is negative when the blade penetrates into the workpiece and is positive when the blade separated from the workpiece.

According to the law of kinematics, force is defined as the change in momentum with respect to time. Increase in velocity thus increase the cutting force. The cutting force started to increase with the cutting speed as the tool edges starts to penetrate workpieces until maximum value then gradually drop to zero when the tool edges move in opposite direction and separated from workpieces.

From figure 25, the displacement of blade in one complete ultrasonic cycle is equal to zero. Hence, the displacement of blade is equal to the distance of feed:

$$s(T) = vT = \frac{v}{f} \quad (10)$$

where  $T$  refers to the period of one complete oscillation and  $f$  refers to the frequency. The displacements of both conventional and ultrasonic assisted cutting are equal.

Since the blade edge does not engaged to the workpiece for the whole cutting process, the cutting force will not be a constant value. According to the impulse theorem, the pressure between the blade edge and the workpiece was maximum when the velocity of the blade comes to the highest value. Hence, the average cutting force

during ultrasonic vibration can be calculated by considering the maximum pressure.

(Hu, Yu, Li, & Chen, 2017):

$$F_c = \tau \cdot s \cdot z \cdot \frac{v}{-2\pi f A + v} \quad (11)$$

$$F_c = \tau \cdot v \cdot \frac{1}{f} \cdot z \cdot \frac{v}{-2\pi f A + v} \quad (12)$$

where,  $\tau$  is the shear stress of the cut plane of the workpiece,  $v$  is the cutting speed of the cutting tool,  $z$  is the cutting depth,  $\theta$  is the inclined angle,  $f$  is frequency and  $A$  is the amplitude of vibration.

According to result of the research done by Jelani (1998), regarding on the cutting force required to cut OPF, the cutting force is highly dependent on the cutting angle. The greater the cutting angle, the greater the force required to cut OPF. The cutting force is maximum at cutting angle of  $90^\circ$ . Table 2 shows the parameters and results of the cutting at  $90^\circ$ .

| Maximum cutting force (kg) | Maximum specific cutting force (kg/cm <sup>2</sup> ) | Cutting depth (cm) | Cutting speed (cm/s) |
|----------------------------|--|--------------------|----------------------|
| 225.87                     | 9.36   | 5.48               | 60                   |

Table 2: Parameters and result of 90o cutting (Jelani, 1998).

## Chapter 4 Result and Discussion

### 4.1 Horn Design

The longitudinal vibration velocity of the aluminium,  $c= 6199\text{m/s}$ , and wavelength,  $\lambda=0.2214\text{m}$  when the natural frequency is  $28\text{kHz}$ . The length of the horns,  $L$  calculated according to equation (5) is  $111\text{mm}$ . The length of horns is affected by the elasticity characteristics of horn material. These characteristics not only affects the efficiency and effectiveness of the vibration transmission, but also the stress distribution and stiffness of the horn.

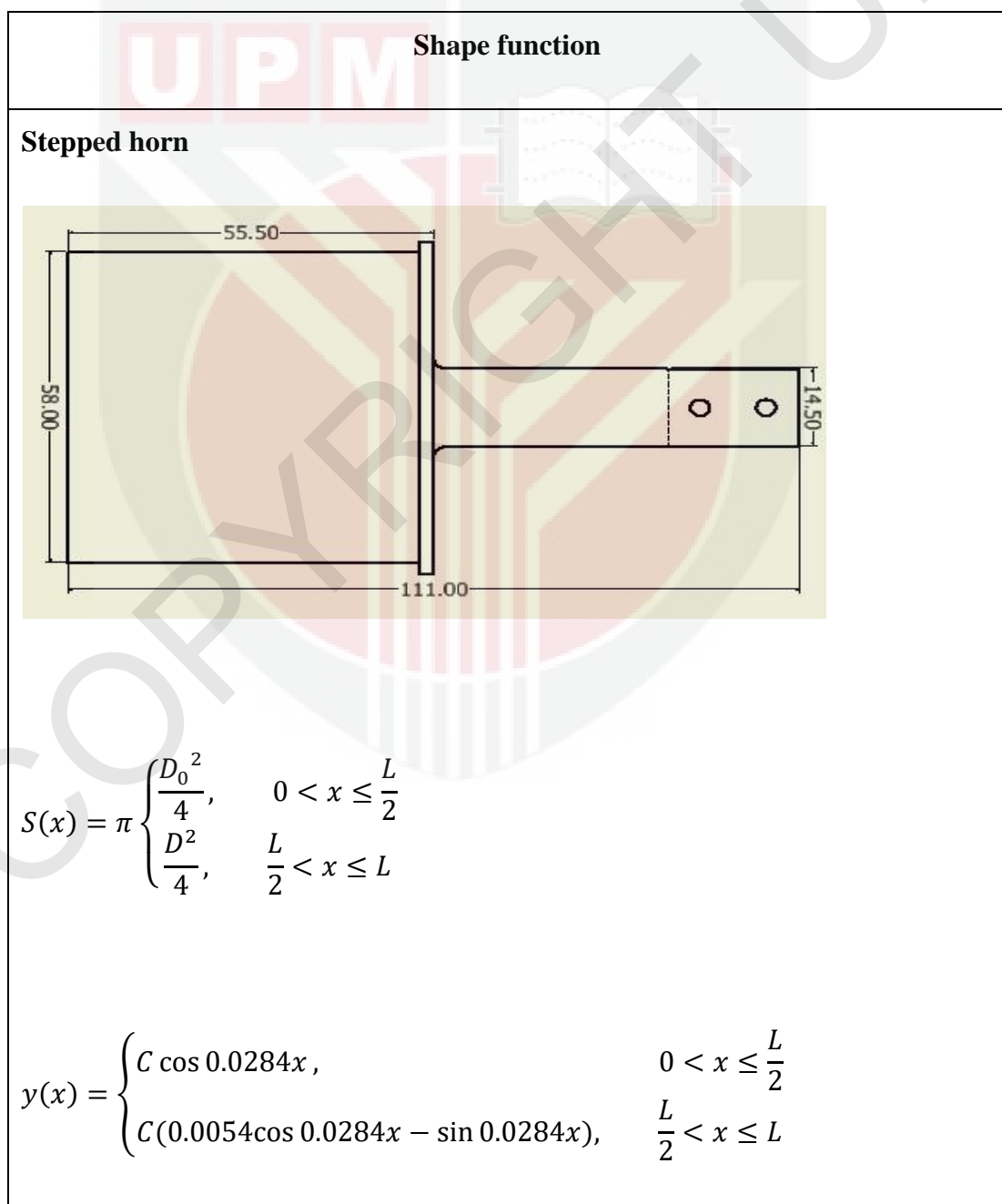
The horns were designed with same features. A  $2\text{mm}$  ridge was designed on step of each horn in order to mount the horn on the test bed. Threaded hole was located at the input end of the horns to connect with ultrasonic transducer with coupling stud.  $2\text{mm}$  thick space at the output end of the horn for slotting of blade. Blade will be fixed vertically on the horn by two bolts and nuts.

The shape functions of each horn are shown in table 3. Substituting the area function into equation (1), we obtained equation x and its solution:

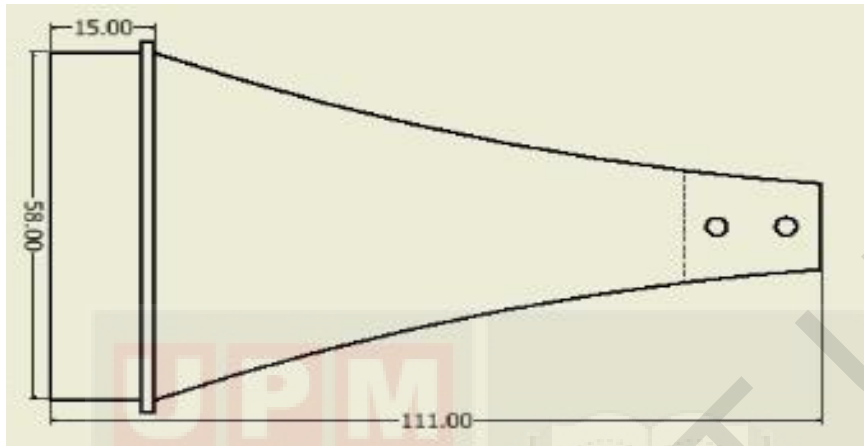
$$y'' + \frac{S'}{S}y' + \frac{\omega^2}{c^2} = 0 \quad (13)$$

$$y(x) = e^{\alpha x} [C_1 \cos \beta x + C_2 \sin \beta x] \quad (14)$$

where  $\alpha + \beta i$  and/or  $\alpha - \beta i$  are the roots of equation x, and  $\omega/c = 0.0284 \text{ rad/mm}$ . The solution of each horn design was solved by applying the boundary conditions.



### Exponential horn

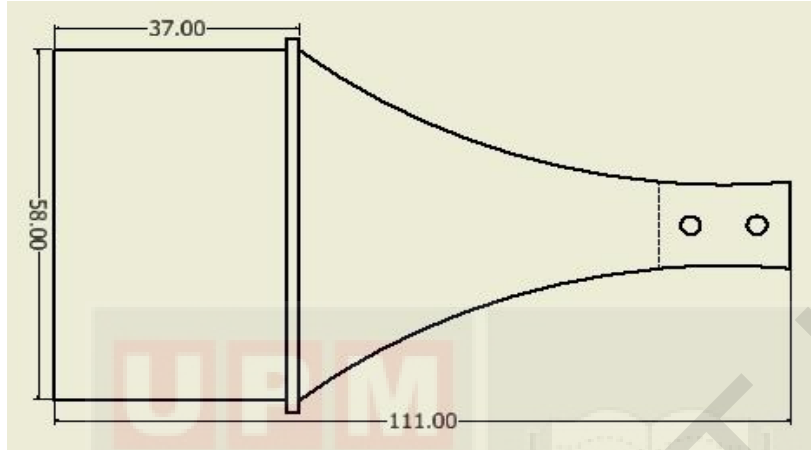


$$S(x) = \pi \begin{cases} \frac{D_0^2}{4}, & 0 < x \leq 15 \\ \frac{D_0^2}{4} e^{-\frac{\ln(D/D_0)}{48}(x-15)}, & 15 < x \leq L \end{cases}$$

$y(x)$

$$= \begin{cases} C \cos 0.0284x, & 0 < x \leq 15 \\ C e^{-0.0145x} (0.9106 \cos 0.0244x - 0.2456 \sin 0.0244x), & 15 < x \leq L \end{cases}$$

### Catenoidal horn



$$S(x) = \pi \begin{cases} \frac{D_0^2}{4}, & 0 < x \leq 37 \\ \frac{D_0^2}{4[0.0405(x-37)+1]}, & 37 < x \leq L \end{cases}$$

$$y(x) \begin{cases} C \cos 0.0284x, & 0 < x \leq 37 \\ C e^{\frac{0.0405x}{0.081x+2}} (0.7154 \cos \gamma(x) - 0.019 \sin \gamma(x)), & 37 < x \leq L \end{cases}$$

where

$$\gamma(x) = \frac{x \sqrt{0.0032 - \frac{0.0016}{0.0405x+1}}}{2}$$

$$D_0 = 58\text{mm}; D = 14.5\text{mm}; L = 111\text{mm}$$

Table 3: Geometry parameters of horns.

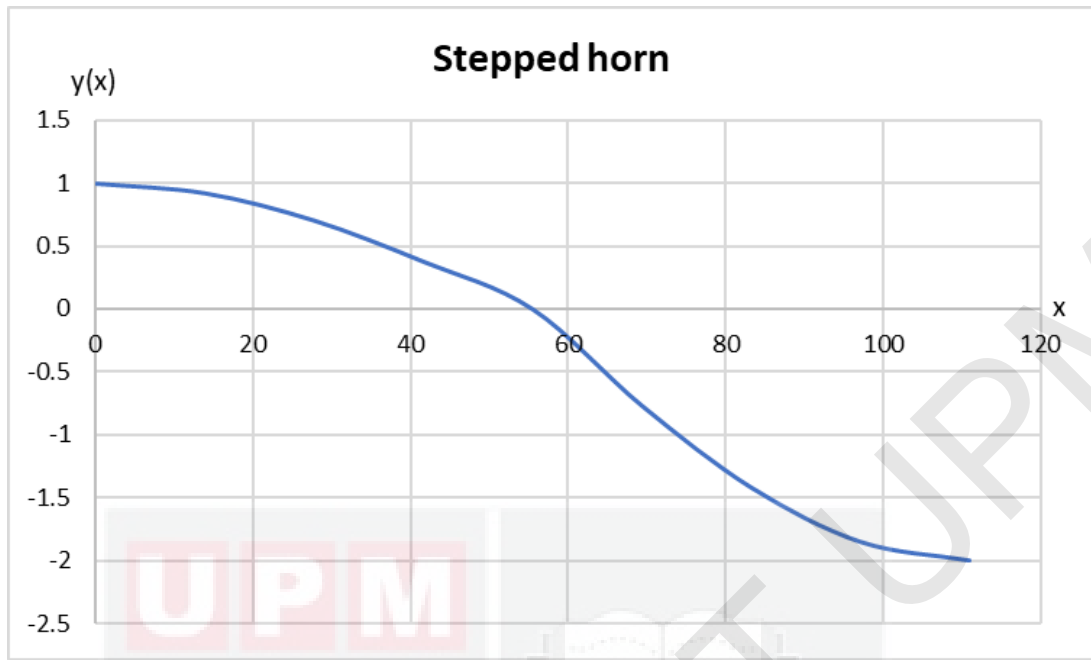


Figure 26: Longitudinal amplitude across stepped horn.

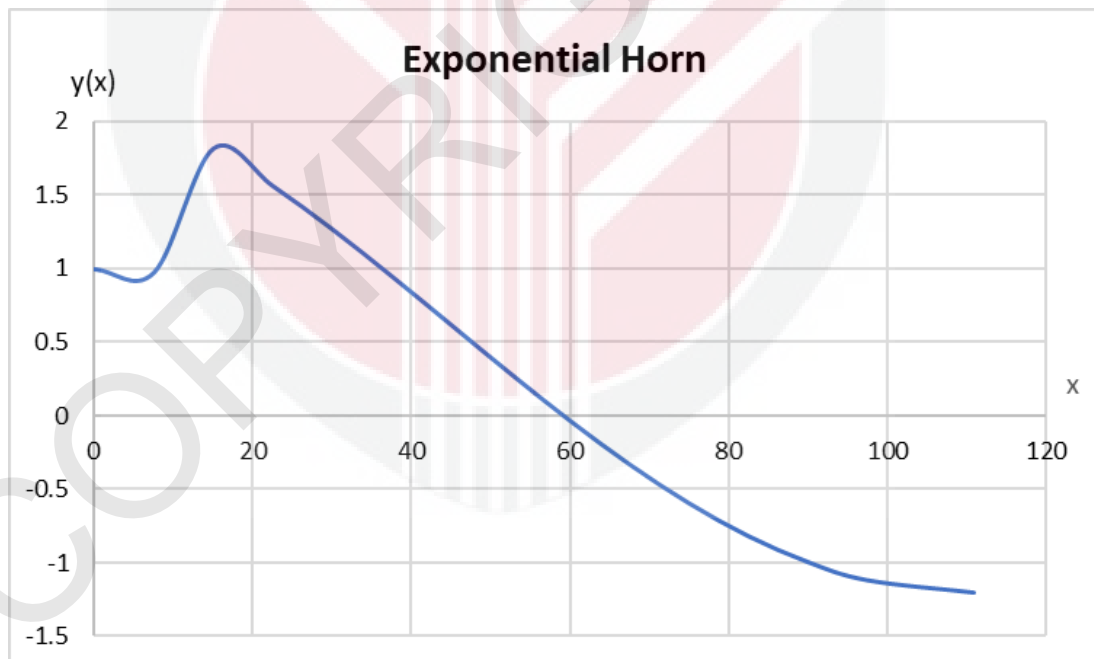


Figure 27: Longitudinal amplitude across exponential horn.

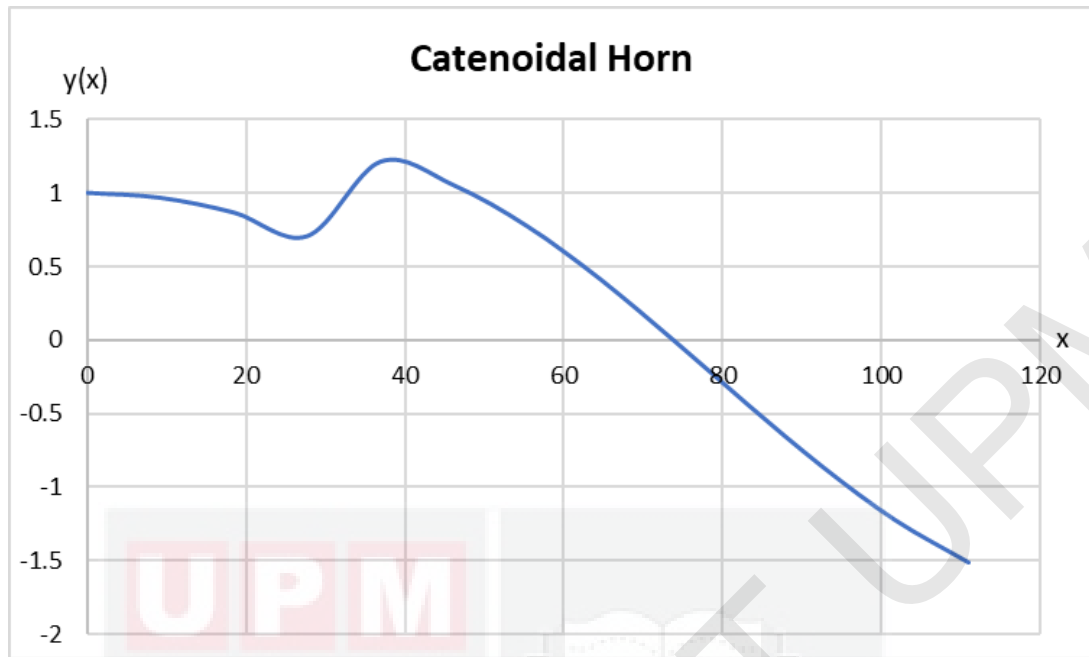


Figure 28: Longitudinal amplitude across catenoidal horn.

Figure 26-28 shows the performance of the horns across the length. The amplification factor of each horn design calculated from equation (7) was tabulated in table 4.

| Horn design      | Amplification factor, M |
|------------------|-------------------------|
| Stepped horn     | 2                       |
| Exponential horn | 1.202                   |
| Catenoidal horn  | 1.513                   |

Table 4: Amplification factor

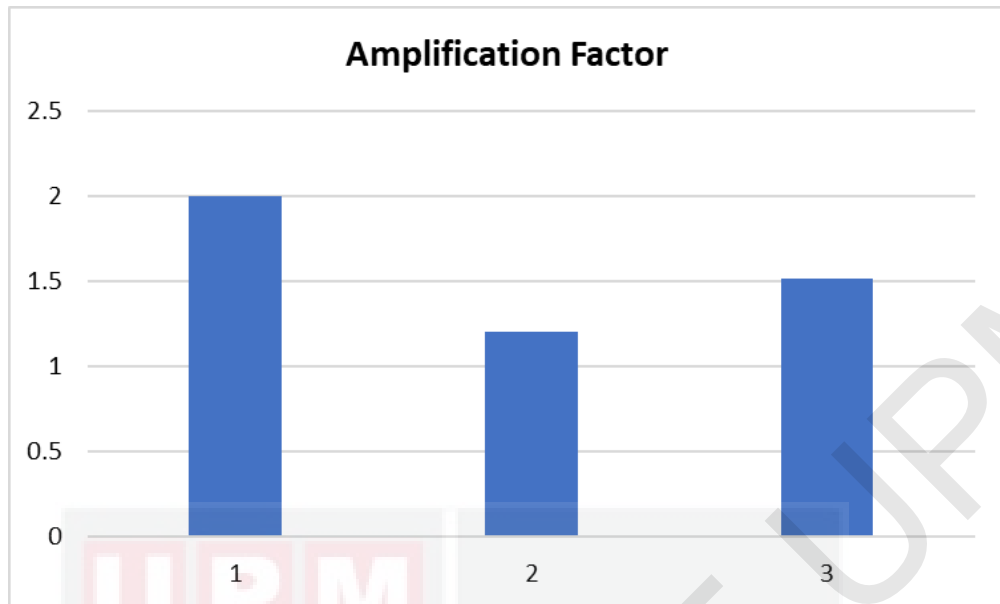


Figure 29: Amplification factor of horns (1:Stepped horn; 2:Exponential horn; 3:Catenoidal horn)

From figure 29, amplification factor of stepped horn was the greatest. The sudden change of the horn diameter concentrates and amplifies the vibration amplitude. As shown in figure 26, the vibration node exists at the step, where the amplitude at this coordinate was equals to zero. From the solution of the longitudinal amplitude function, we can see that the diameter change of the horn has no effect to the amplitude as the diameter before and after step change of the horn were constant throughout the horn. Hence, the performance of a stepped horn depends on the position of step change. Although the amplification characteristic of stepped horn was the best among these three designs, however, the sudden change in area across the horn may cause failure due to exceed of maximum allowable stress.

The amplification factor of exponential horn was the smallest. The gradual taper shape of the horn amplifies the vibration gradually. The amplifying performance

of exponential horn is relatively lower than stepped horn because the diameter of the horn reduces gradually across the horn. However, this shape characteristic allows better internal stress distribution. The performance of exponential horn depends on the exponential function parameter of the horn geometry. The greater the curve of the taper surface, the greater the amplifying performance. However, this also indicates the horn will have a weaker stress distribution performance.

Catenoidal horn has an amplification factor in between stepped horn and exponential horn. This condition also indicates that catenoidal horn has better stress distribution than stepped horn and better amplifying performance than exponential horn. The curvature of the catenoidal horn was greater than exponential horn. As such, it can concentrate and amplifies the vibration better than exponential horn yet performing better stress distribution than stepped horn. Same as exponential horn, the performance of catenoidal horn depends on its shape parameter, which determines the curvature of the horn.

## 4.2 Horn Tuning

The result of the horn tuning experiment was tabulated in table 5. The comparison of the resonant frequency was shown in figure 30.




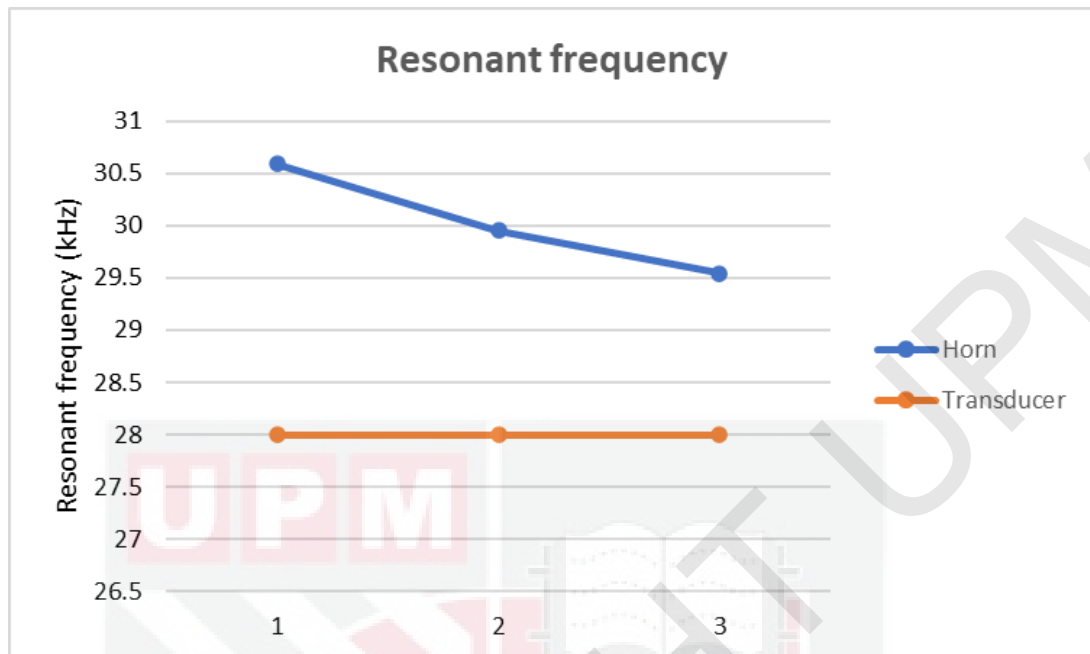
| <b>Horn</b>   | <b>Resonant frequency (kHz)</b> | <b>Difference of resonant frequency (kHz)</b> |
|---|---------------------------------|---|
| Bare transducer   | 28                              | -   |
| Step horn<br>         | 30.59                           | 2.59  |
| Exponential horn<br> | 29.95                           | 1.95  |
| Catenoidal horn<br>  | 29.54                           | 1.54  |

Table 5: Resonant frequency



*Figure 30: Comparison of resonant frequency.*

From the result, the frequency required for the horn assembly to achieve resonant state was the highest from stepped horn, followed by exponential horn and catenoidal horn. The resonant frequencies of three horn design was not much difference. This is because all three horns are fabricated from same material, which is aluminium and having same length and diameter. According to Nad (2010), the natural frequency of horn was dependant on the physical characteristic of horn material and the length of the horn. Since, all horns in this experiment having equal length and material, geometry of the horn was the only factor affecting the horn performance.

Catenoidal horn has the nearest resonant frequency to the natural frequency of bare ultrasonic transducer. Horn with the nearest resonant frequency would able to oscillate with greatest vibration amplitude as it is close to the resonant state which

provides maximum vibration amplitude. Catenoidal horn combines both amplifying and better stress distribution characteristics of stepped horn and exponential horn. As mentioned in section before, the curvature of horn shape affects the amplifying and stress distribution performance. High amplifying characteristic can improve the cutting performance and good stress distribution reduce failure at the horn. Catenoidal horn has a greater curved surface than exponential horn yet having gradual decrease in surface, hence able to perform both amplifying and stress distribution well. In the nutshell, catenoidal horn is the most suitable horn design as amplifier in ultrasonic cutting.

### 4.3 Cutting Force Requirement

By substituting the parameters of OPF cutting at 90° from table 2 into equation (12), the cutting force equation was:

$$F_c = \frac{184654.08}{-2\pi f^2 A + 60f} \quad (15)$$

Using the partial differentiation method, the equation can be solved into:

$$\frac{\partial F}{\partial f} = \frac{738616.32\pi f A - 11079244.8}{(-2\pi f^2 A + 60f)^2} = 0 \quad (16)$$

$$f = \frac{4.775}{A} \quad (17)$$

$$\frac{\partial^2 F}{\partial^2 f} > 0 \Rightarrow F \text{ is maximum when } f = \frac{4.775}{A} \quad (18)$$

and

$$\frac{\partial F}{\partial A} = \frac{369308.16f^2}{(-2\pi f^2 A + 60f)^2} = 0 \Rightarrow \text{unable to solve} \quad (19)$$

Substitute equation (17) into equation (15), we get:

$$F_c = \frac{6155.14}{f} \quad (20)$$

where  $F_c$  in kg, and  $f$  in Hz.

From partial differential equation (16), such relationship of frequency and amplitude in equation (17) will give the maximum cutting force. The equation shows that the frequency is inversely proportional to the vibration amplitude. Vibration frequency should be constant for the entire cutting system, but the amplitude can be varied using different horns with specific amplification magnitude. The final equation (20) solved shows how the cutting force varies with the vibration frequency. The higher the vibration frequency, the lower the force required to cut the frond.

The common range of ultrasonic transducer used in wood industry is 20kHz-40kHz. Assuming the effect of damping is not noticeable, the cutting force required to cut OPF when the cutting process is assisted with 20kHz ultrasonic vibration is 0.3078kg which is much lower than the cutting without ultrasonic vibration (225.87kg). However, the reduction of cutting force required might be much lower than the calculated value due to structural damping and friction during the cutting process.

Partial differential equation (19) was unable to be solved. This indicates that the cutting force is not depends solely on the amplitude of vibration. Both frequency and amplitude of vibration having significant effect on the cutting force developed on the cutting tip. However, it is difficult to obtain the perfect ratio of frequency and amplitude in practice. This is because the vibration delivered to the cutting end always having smaller value due to the damping effect, as such reduce the force developed at the cutting edge.

#### **4.4 Comparison with Current Oil Palm Cutter**

The main components of the motorised cutter are cutting head, gear set, telescopic shaft and bearings. Mechanical vibration was transmitted from the motor to the cutting head via the shaft and the connecting components. Hence, high amplitude vibration will be induced to the user along the pole. For ultrasonic actuating mechanism, the cutting head is vibrated with high frequency ultrasonic vibration. This mechanism allows cutting with relatively low amplitude vibration. Also, the cutting head is connected directly to the transducer, thus zero or only low vibration will be induced to the user via the pole.

Battery powered electric cutter allow high speed cutting with reduced moving parts. Hence, the electric cutter enables good cutting experience with low vibration and low noise emission. The ultrasonic actuating mechanism has the similar advantages as the vibration is directly transmitted to the cutting head and the actuator is held on a pole. Ultrasonic actuating mechanism provide high frequency vibration

hence reducing more cutting force required to be applied by the user during the operation. Hence, it is assumed that the ultrasonic actuating mechanism can improve the efficiency of cutting.



## Chapter 5 Conclusion and Recommendations

Three horns with different design was fabricated. The horn design having best performance in terms of amplification factor was stepped horn. However, the result of the horn tuning experiment shows that catenoidal horn can perform better due to its characteristics of both amplifying and stress distribution. The equation showing the relationship between the natural frequency, vibration amplitude and the cutting force was derived. When high frequency vibration induced to the cutting tool, lower cutting force are required to perform cutting. On the other hand, higher frequency actuator will induce lower vibration amplitude. The objectives of this project were achieved.

Due to the large size and dense mass of sickle, the horn's output diameter where sickle connected to should be large enough to support the sickle. In order to achieve the same amplifying magnitude, the horn's input diameter should be large enough as well. This requires large size transducer which has the compatible matching diameter. However, the size of Langevin transducers available in the market are not large enough, therefore, customisation of the actuator may be required to fabricate the ultrasonic oil palm trimmer. Besides, there may be losses during the vibration transmission from the horn's end to the sickle's blade edge. As such, the mechanical properties of the sickle should be taken into account when designing the whole ultrasonic oil palm cutting device.

## Chapter 6 Summary

The findings of this project can be summarized into four points. First, the most suitable horn design for amplifying vibration amplitude is catenoidal horn. The amplification magnitude varied according to the curvature of the concave surface of the horn. Second, the length of the horn depends on the mechanical characteristics of the horn material. In this case, a shorter horn is more suitable to support the mass of the sickle. Third, the ultrasonic frequency is inversely proportional to the vibration amplitude where the amplitude can be amplified by the horn. Lastly, the cutting force required to cut an oil palm frond is inversely proportional to the ultrasonic frequency. A higher frequency actuator saves more force for cutting.

## References

- Abdullah, M. Z., Guan, L. C., Lim, K. C., & Karim, A. A. (2004). The applications of computer vision system and tomographic radar imaging for assessing physical properties of food. *Journal of Food Engineering*, 61(1 SPEC.), 125–135. [https://doi.org/10.1016/S0260-8774\(03\)00194-8](https://doi.org/10.1016/S0260-8774(03)00194-8)
- Ahmad, D., & Hitam, A. (1999). *90°J 60°*. 11(2), 114–122.
- Ahmad, M. R., Ikmal, M., Azaman, H., Shuib, A. R., Khalid, M. R., Bakri, A., ... Ramli, A. S. (2020). *Battery Driven Harvesting Tool ( Cantas Elektro ). 1*, 1–8.
- Alnuami, W., Janius, R. B., & Ahmad, D. (2015). *Factors Affecting the Mechanical Strengths of Oil Palm Fronds*. 4(3), 138–149.
- Amin, S. G., Ahmed, M. H. M., & Youssef, H. A. (1995). Computer-aided design of acoustic horns for ultrasonic machining using finite-element analysis. *Journal of Materials Processing Tech.*, 55(3–4), 254–260. [https://doi.org/10.1016/0924-0136\(95\)02015-2](https://doi.org/10.1016/0924-0136(95)02015-2)
- Azhar, F., Norhisam, M., Wakiwaka, H., Tashiro, K., & Nirei, M. (2012). Current Achievement and Future Plan for Improvement for E Cutter Development. *The 24th Symposium on Electromagnetics and Dynamics, SEAD 24*, (May), 1–6. <https://doi.org/10.13140/2.1.3540.3048>
- Babitsky, V. I., Kalashnikov, A. N., & Molodtsov, F. V. (2004). Autoresonant control of ultrasonically assisted cutting. *Mechatronics*, 14(1), 91–114. [https://doi.org/10.1016/S0957-4158\(03\)00014-X](https://doi.org/10.1016/S0957-4158(03)00014-X)
- Bulan, R., Mandang, T., & Hermawan, W. (2015). *Physical and Mechanical Properties of Palm Frond for the Development of Palm Oil Waste Chopper and Pressing Machine Design*. 6(2), 117–120.
- Cardoni, A., & Lucas, M. (2002). Enhanced vibration performance of ultrasonic block horns. *Ultrasonics*, 40(1–8), 365–369. [https://doi.org/10.1016/S0041-624X\(02\)00123-3](https://doi.org/10.1016/S0041-624X(02)00123-3)
- Chowdhry, R., & Sethi, V. (2017). Hand arm vibration syndrome in dentistry: A review. *Current Medicine Research and Practice*, 7(6), 235–239. <https://doi.org/10.1016/j.cmrp.2017.11.001>
- Darwis, A., Massijaya, M. Y., Nugroho, N., Alamsyah, E. M., & Nurrochmat, D. R. (2014). Bond ability of oil palm xylem with isocyanate adhesive. *Jurnal Ilmu Dan Teknologi Kayu Tropis*, 12(1), 39–47. Retrieved from <http://ejournalmapeki.org/index.php/JITKT/article/view/81>
- Dong, W., Anish, R., & V, S. V. (2020). *Production of high-quality extremely-thin histological sections by ultrasonically assisted cutting*. 276(April 2019). <https://doi.org/10.1016/j.jmatprotec.2019.116403>
- Han, X., Zhang, D., & Song, G. (2019). Review on current situation and development trend for ultrasonic vibration cutting technology. *Materials Today: Proceedings*, (xxxx). <https://doi.org/10.1016/j.matpr.2019.07.715>
- Hu, X. P., Yu, B. H., Li, X. Y., & Chen, N. C. (2017a). *Research on Cutting Force Model of Triangular Blade for Ultrasonic Assisted Cutting Honeycomb*

- Composites*, 66, 159–163. <https://doi.org/10.1016/j.procir.2017.03.283>
- Hu, X. P., Yu, B. H., Li, X. Y., & Chen, N. C. (2017b). Research on Cutting Force Model of Triangular Blade for Ultrasonic Assisted Cutting Honeycomb Composites. *Procedia CIRP*, 66, 159–163. <https://doi.org/10.1016/j.procir.2017.03.283>
- Jelani, A. R., Ahmad, M. R., Azaman, M. I. H., Gono, Y., Mohamed, Z., Sukawai, S., ... Kushairi, A. (2018). Development and evaluation of a new generation oil palm motorised cutter (cantas Evo). *Journal of Oil Palm Research*, 30(2), 276–288. <https://doi.org/10.21894/jopr.2018.0015>
- Jelani, A. R., Hitam, A., Jamak, J., Noor, M., Gono, Y., & Ariffin, O. (2008). Cantas<sup>TM</sup> - A tool for the efficient harvesting of oil palm fresh fruit bunches. *Journal of Oil Palm Research*, 20(DECEMBER), 548–558.
- Jin, M., & Murakawa, M. (2001). Development of a practical ultrasonic vibration cutting tool system. *Journal of Materials Processing Technology*, 113(1–3), 342–347. [https://doi.org/10.1016/S0924-0136\(01\)00649-5](https://doi.org/10.1016/S0924-0136(01)00649-5)
- Karafi, M. R., & Khorasani, F. (2019). Evaluation of mechanical and electric power losses in a typical piezoelectric ultrasonic transducer. *Sensors and Actuators, A: Physical*, 288, 156–164. <https://doi.org/10.1016/j.sna.2018.12.044>
- Lu, X., Hu, J., Peng, H., & Wang, Y. (2017). A new topological structure for the Langevin-type ultrasonic transducer. *Ultrasonics*, 75, 1–8. <https://doi.org/10.1016/j.ultras.2016.11.008>
- Lucas, M., Petzing, J. N., Cardoni, A., & Smith, L. J. (2001). Design and characterisation of ultrasonic cutting tools. *CIRP Annals - Manufacturing Technology*, 50(1), 149–152. [https://doi.org/10.1016/S0007-8506\(07\)62092-7](https://doi.org/10.1016/S0007-8506(07)62092-7)
- Macaire, W. H., Bernard, T., Noel, T., Felicite, T. M., Cesar, K., Michel, L., & Jacques, F. (2010). Extraction of Palm Kernel Oil in Cameroon: Effects of Kernels Drying on the Oil Quality. *Journal of Food Technology*, 8(1), 1–7. <https://doi.org/10.3923/jftech.2010.1.7>
- Mandang, T., Sinambela, R., & Pandianuraga, N. R. (2018). Physical and mechanical characteristics of oil palm leaf and fruits bunch stalks for bio-mulching. *IOP Conference Series: Earth and Environmental Science*, 196(1). <https://doi.org/10.1088/1755-1315/196/1/012015>
- Nad, M. (2010). Ultrasonic horn design for ultrasonic machining technologies. *Applied and Computational Mechanics*, 4(1), 79–88.
- Palm, M., Board, O., & Ahmad, D. (1998). Force and energy requirement for cutting oil palm fronds. *Journal of Oil Palm Research*, 10(December 1998), 10–24.
- Pérez-Sánchez, A., Segura, J. A., Rubio-Gonzalez, C., Baldenegro-Pérez, L. A., & Soto-Cajiga, J. A. (2020). Numerical design and analysis of a langevin power ultrasonic transducer for acoustic cavitation generation. *Sensors and Actuators, A: Physical*, 311. <https://doi.org/10.1016/j.sna.2020.112035>
- Rincón, S. M., Hormaza, P. A., Moreno, L. P., Prada, F., Portillo, D. J., García, J. A., & Romero, H. M. (2013). Use of phenological stages of the fruits and physicochemical characteristics of the oil to determine the optimal harvest time of oil palm interspecific OxG hybrid fruits. *Industrial Crops and Products*, 49, 204–210. <https://doi.org/10.1016/j.indcrop.2013.04.035>

- Schneider, Y., Zahn, S., & Rohm, H. (2008). Power requirements of the high-frequency generator in ultrasonic cutting of foods. *Journal of Food Engineering*, 86(1), 61–67. <https://doi.org/10.1016/j.jfoodeng.2007.09.024>
- Shuib, A. R., Mohd, :, Khalid, R., & Deraman, M. S. (2010). Enhancing Field Mechanization in Oil Palm Management. *Oil Palm Bulletin*, 61(October 2016), 1–10.
- Sinn, G., Zettl, B., Mayer, H., & Stanzl-Tschegg, S. (2005). Ultrasonic-assisted cutting of wood. *Journal of Materials Processing Technology*, 170(1–2), 42–49. <https://doi.org/10.1016/j.jmatprotec.2005.04.076>
- Vivekananda, K., Arka, G. N., & Sahoo, S. K. (2014). Design and analysis of ultrasonic vibratory tool (UVT) using FEM, and experimental study on Ultrasonic Vibration-assisted turning (UAT). *Procedia Engineering*, 97, 1178–1186. <https://doi.org/10.1016/j.proeng.2014.12.396>
- Yamaguchi, D., Kanda, T., & Suzumori, K. (2012). An ultrasonic motor for cryogenic temperature using bolt-clamped Langevin-type transducer. *Sensors and Actuators, A: Physical*, 184, 134–140. <https://doi.org/10.1016/j.sna.2012.06.024>
- Zahn, S., Schneider, Y., & Rohm, H. (2006). Ultrasonic cutting of foods: Effects of excitation magnitude and cutting velocity on the reduction of cutting work. *Innovative Food Science and Emerging Technologies*, 7(4), 288–293. <https://doi.org/10.1016/j.ifset.2006.04.004>
- Ng, S. k. (1957). *The oil palm: Its culture, manuring and utilisation*. Switzerland: Potash Institute.
- Henson, I.E. (2002) Oil palm pruning and relationships between leaf area and yield: a review of previous experiments. *The Planter, Kuala Lumpur* 78(916):351–362.
- Rawson, F. F. (1998). An introduction to ultrasonic food cutting. In M. J. W. Povey & T.J. Mason (Eds.), *Ultrasound in food processing* (pp. 254–269). London: Blackie Academic.
- Mitrofanov, A.V., Babitsky, V.I. & Silberschmidt, V.V. (2003). Finite element simulations of ultrasonically assisted turning. *Computational Materials Science*, 28, 645–653.
- Cheng, X.L., Zhao, B., Liu, C.S., Jiao, F., Gao, G.F. (2007). *Coal Mine Mach.* 28 (1), 104–105.
- Yang, L.& Lu, Z.S. (2007). *Manufacture Technology Machine Tool* 3, 92–96.



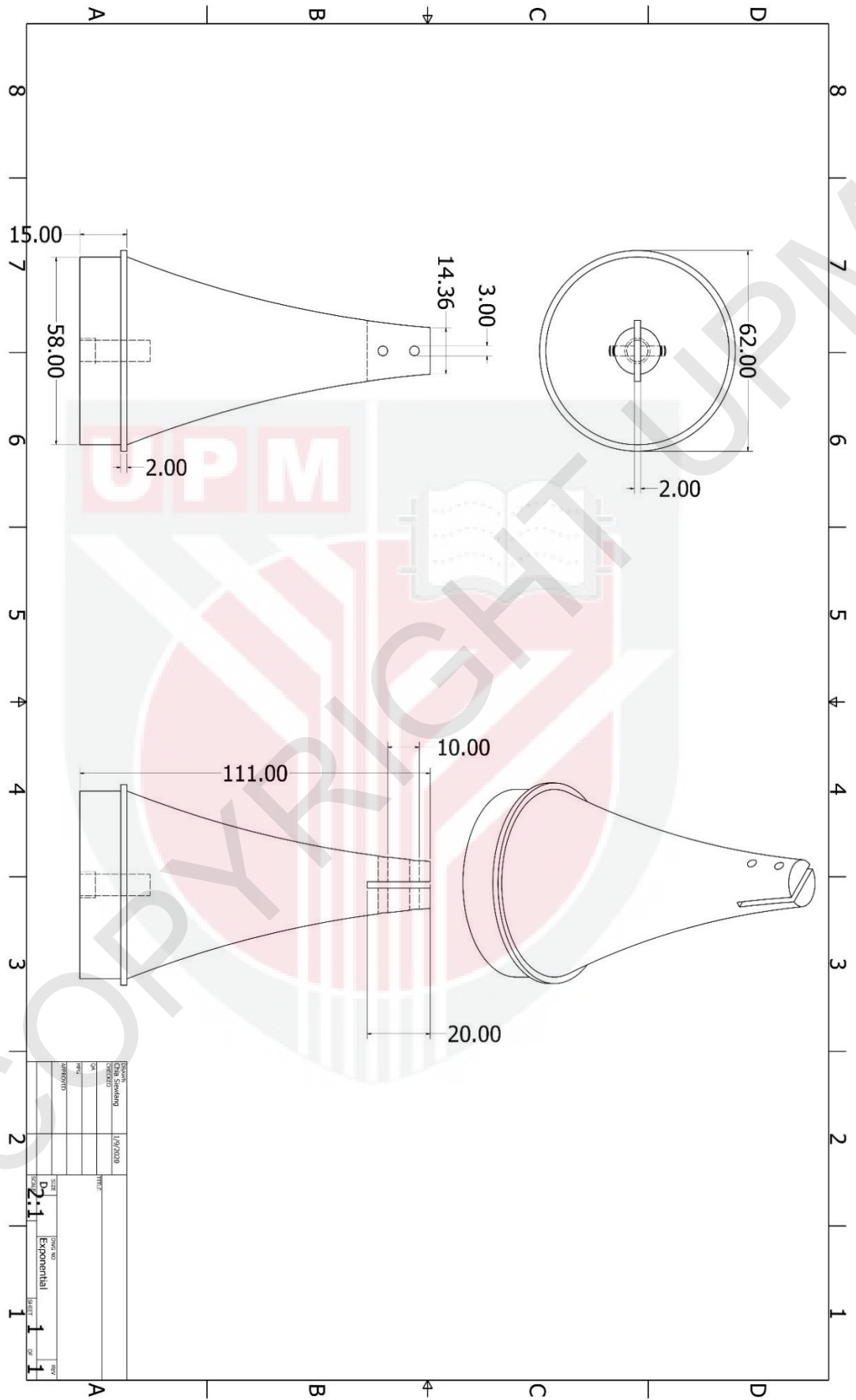


Figure 32: Exponential horn

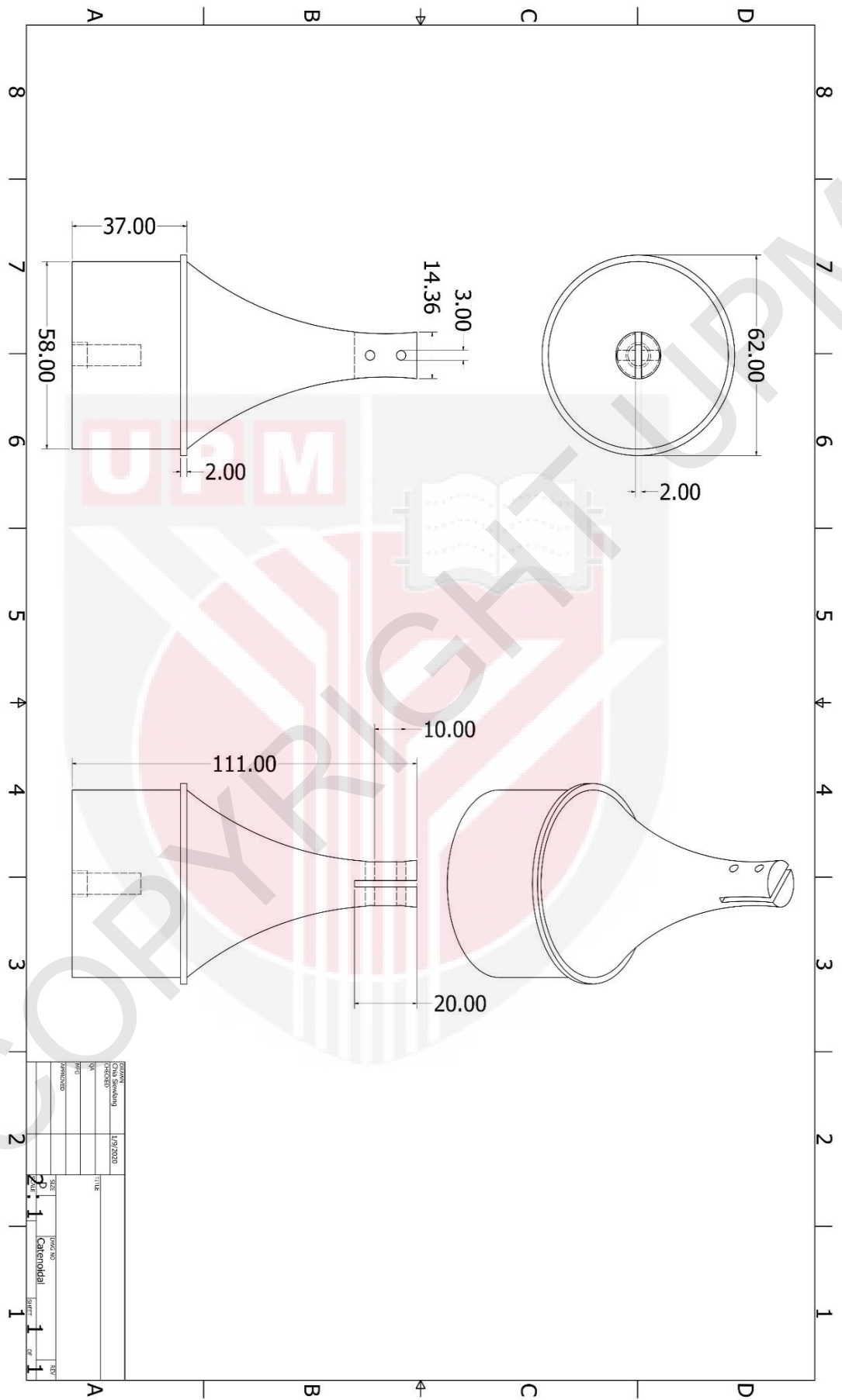


Figure 33: Catenoidal horn

| <b>Longitudinal coordinate, x (mm)</b> | <b>Longitudinal amplitude, y (mm)</b> |
|--|---------------------------------------|
| 0                                      | 1                                     |
| 13.875                                 | 0.9234                                |
| 27.75                                  | 0.7052                                |
| 41.625                                 | 0.378936043                           |
| 55.5                                   | 0                                     |
| 69.375                                 | -0.7679                               |
| 83.25                                  | -1.4189                               |
| 97.125                                 | -1.85089                              |
| 111                                    | -2                                    |

*Table 6: Longitudinal amplitude across stepped horn.*

| <b>Longitudinal coordinate, x (mm)</b> | <b>Longitudinal amplitude, y (mm)</b> |
|--|---------------------------------------|
| 0                                      | 1                                     |
| 7.5                                    | 0.9774                                |
| 15                                     | 1.8212                                |
| 22.5                                   | 1.5657                                |
| 30                                     | 1.2718                                |
| 37.5                                   | 0.9526                                |
| 45                                     | 0.6208                                |
| 52.5                                   | 0.2891                                |
| 60                                     | -0.0307                               |
| 67.5                                   | -0.3277                               |
| 75                                     | -0.5922                               |
| 82.5                                   | -0.8158                               |
| 90                                     | -0.9921                               |
| 97.5                                   | -1.1163                               |
| 111                                    | -1.2015                               |

*Table 7: Longitudinal amplitude across exponential horn.*

| <b>Longitudinal coordinate, x (mm)</b> | <b>Longitudinal amplitude, y (mm)</b> |
|--|---------------------------------------|
| 0                                      | 1                                     |
| 9.25                                   | 0.9657                                |
| 18.5                                   | 0.86517                               |
| 27.75                                  | 0.7052                                |
| 37                                     | 1.2123                                |
| 46.25                                  | 1.0489                                |
| 55.5                                   | 0.7704                                |
| 64.75                                  | 0.4066                                |
| 74                                     | -0.0092                               |
| 83.25                                  | -0.4423                               |
| 92.5                                   | -0.8582                               |
| 101.75                                 | -1.2246                               |
| 111                                    | -1.5135                               |

*Table 8: Longitudinal amplitude across catenoidal horn.*